miR-155 promotes an inflammatory response in HaCaT cells via the IRF2BP2/KLF2/NF-κB pathway in psoriasis

LU CHEN[1*], CHANG LIU[1*], XUESONG XIANG[1*], WENHONG QIU[1] and KAIWEN GUO[2]

[1]Department of Immunology, School of Medicine, Jianghan University, Wuhan, Hubei 430056, P.R. China;
[2]Department of Pathogenic Biology, Medical College, Wuhan University of Science and Technology, Wuhan, Hubei 430065, P.R. China

Received February 1, 2024; Accepted July 16, 2024

DOI: 10.3892/ijmm.2024.5415

Abstract. Psoriasis is a chronic inflammatory skin condition with numerous causes, including genetic, immunological and infectious factors. The course of psoriasis is long and recurrence is common; pathogenesis is not completely understood. However, there is an association between advancement of psoriasis and aberrant microRNA (miR or miRNA)-155 expression. Through bioinformatics, the present study aimed to analyze the differentially expressed genes and miRNAs in psoriasis and its biological mechanism and function psoriatic inflammation. First of all, differentially expressed genes (DEGs) and miRNAs (DEMs) in patients with psoriasis were identified using GEO2R interactive web application. A psoriasis inflammatory model was established using lipopolysaccharide (LPS)-treated HaCaT keratinocytes, which were transfected with miR-155 mimic or inhibitor. Cell Counting Kit-8 was used for the assessment of cell viability and proliferation, and changes in the cell cycle were examined using flow cytometry. ELISA and reverse transcription-quantitative PCR (RT-qPCR) were used to detect the expression levels of the inflammatory factors IL-1β and IL-6. The dual-luciferase reporter assay was used to verify the targeting association between miR-155-5p and IFN regulatory factor 2 binding protein 2 (IRF2BP2). To verify the targeting association of miR-155 and the IRF2BP2/kruppel-like factor 2 (KLF2)/NF-κB signaling pathway, expression levels of IRF2BP2, KLF2 and p65 were identified by RT-qPCR and western blotting. IRF2BP2 levels were also confirmed by immunofluorescence, in conjunction with bioinformatics database analysis. Overexpression of miR-155 inhibited proliferation of HaCaT cells and increased the number of cells in S phase and decreasing number of cells in G1 and G2 phase. In the LPS-induced inflammatory state, miR-155 overexpression heightened the inflammatory response of HaCaT cells while inhibition of miR-155 lessened it. Suppression of inflammatory cytokine expression by miR-155-5p inhibitor was reversed by knockdown of IRF2BP2. miR-155 was shown to interact with IRF2BP2 to negatively regulate its expression, leading to decreased KLF2 expression and increased p65 expression and secretion of inflammatory factors, intensifying the inflammatory response of HaCaT cells. Therefore, miR-155 may contribute to development of psoriasis by inducing tissue and cell damage by increasing the inflammatory response of HaCaT cells via the IRF2BP2/KLF2/NF-κB pathway. In conclusion, the results of the present study offer novel perspectives on the role of miR-155 in the onset and progression of psoriasis.

Introduction

Numerous causes, including genetic, immunological and viral, can induce psoriasis, a common chronic inflammatory skin condition (1). Furthermore, there are multiple cytokine imbalances and intracellular signal transduction abnormalities in the onset of psoriasis. Psoriasis is linked to excessive activation of neutrophils, dendritic and T cells and keratinocytes, resulting in proliferation of the epidermal spinous layer, hyperkeratosis and parakeratosis, disappearance of the granular layer and epidermal microabscesses (1-3).

Psoriatic arthritis, lymphadenitis and cardiovascular disorders are among the side effects of severe psoriasis (1,4,5). The long-term nature and recurrence of the condition imposes a burden on the lives and wellbeing of patients. Although there is no cure for psoriasis, numerous targeted therapies effectively alleviate symptoms or slow their progression, including TNF-α inhibitors etanercept, adalimumab and infliximab (1). Identifying disease biomarkers may aid personalized treatment methods to maximize therapeutic effects.

microRNAs (miRNAs or miRs) are highly conserved non-coding RNAs that are key post-transcriptional epigenetic factors. miRNAs are involved in translational regulation, either by binding to target mRNA to degrade it or by physically

Correspondence to: Dr Wenhong Qiu, Department of Immunology, School of Medicine, Jianghan University, 8 Sanjiaohu Road, Caidian, Wuhan, Hubei 430056, P.R. China
E-mail: qiuwenhong@jhun.edu.cn

Dr Kaiwen Guo, Department of Pathogenic Biology, Medical College, Wuhan University of Science and Technology, 2 Huangjiahu West Road, Hongshan, Wuhan, Hubei 430065, P.R. China
E-mail: guowendy@wust.edu.cn

*Contributed equally

Key words: microRNA-155, psoriasis, IFN regulatory factor 2 binding protein 2, NF-κB, inflammatory response, biomarker

blocking transcription factors to prevent protein synthesis (6). By controlling keratinocyte differentiation and hyperplasia, triggering apoptosis and immunological activation, miRNAs can be crucial in psoriasis (7). miRNAs have been proven to be effective biomarkers for psoriasis diagnosis, prognosis and therapy monitoring (8). Upregulation of miR-155 can disrupt normal epidermal barrier formation by lowering loricrin (a protein component of the keratinocyte envelope) production in keratinocytes in a human external skin model (9). There is also evidence that skin lesions and peripheral blood mononuclear cells of patients with psoriasis have higher miR-155 expression levels, which is key for the proliferation, programmed cell death and inflammatory response of HaCaT cells. miR-155 may therefore have a key role in the pathophysiology of psoriasis (10,11).

As a transcriptional corepressor, IFN regulatory factor 2 binding protein 2 (IRF2BP2) inhibits basal transcription and suppresses enhancer activation and gene expression (12). IRF2BP2 is widely expressed in different types of cell and tissue, such as bone marrow, skin, liver, dendritic cells, basophil cells, and naive CD4 T cells, potentially influencing cellular signaling pathways (13). IRF2BP2 has a role in maintaining physiological cell homeostasis by controlling cellular processes, including angiogenesis, inflammation, cell cycle and the immune response (12,14,15).

Furthermore, studies have demonstrated the importance of IRF2BP2 in controlling the inflammatory process (12,16-20). IRF2BP2 has a critical role in macrophage-mediated inflammation. Chen *et al* (16) confirmed that upregulation of IRF2BP2 regulates expression of kruppel-like factor 2 (KLF2), an anti-inflammatory transcription factor, and promotes M2 macrophage differentiation. Moreover, via suppressing NF-κB activation, IRF2BP2 upregulation in the heart decreases the synthesis of pro-inflammatory cytokines (20). However, it is unclear how IRF2BP2 contributes to the inflammatory response in psoriasis.

Bioinformatics enrichment tools have served a key role in analyzing gene function and identifying potential regulatory mechanisms of gene networks in high-throughput biological studies (21-23). By using bioinformatics data mining, key genes associated with diseases can be efficiently identified, promoting understanding of disease pathogenesis. Furthermore, effective biomarkers or targets can be utilized to aid in patient diagnosis and treatment.

The aim of the present study was to screen differentially expressed genes and differentially expressed miRNAs in psoriasis by bioinformatics and to explore the role of miR-155 in the occurrence and development of the psoriasis inflammatory response and its molecular mechanism, which may provide a new approach for targeted treatment of this disease.

Materials and methods

Microarray. A total of four datasets (GSE166388, GSE153007, GSE115293 and GSE145305) that included gene expression profiles from patients with psoriasis and healthy controls were obtained from The Gene Expression Omnibus (GEO) database (ncbi.nlm.nih.gov/geo). The mRNA expression profiles of four psoriasis and four normal samples were included in the GSE166388 microarray dataset, whereas the mRNA expression profiles of 14 psoriasis and five normal samples were included in GSE153007. GSE115293 and GSE145305 both contained miRNA expression profiles from four psoriasis and four normal samples. The psoriasis samples were obtained from biopsy of diseased skin from patients with psoriasis and the control samples were obtained from biopsy of normal skin from healthy volunteers.

Identification of differentially expressed genes (DEGs) and miRNAs (DEMs). DEGs and DEMs were identified using GEO2R (ncbi.nlm.nih.gov/geo/geo2r/), an interactive web application that compares samples from GEO database to identify DEGs. The screening criteria for DEGs and DEMs were $P<0.05$ and $|\log\text{Fold-change}|\geq 1$. Using online bioinformatics tool ChiPlot (chiplot.online/), data were presented as heat maps and volcano plots. GSE166388 and GSE153007 datasets were used to obtain mRNAs and the GSE115293 and GSE145305 datasets were used to obtain miRNAs associated with psoriasis. The online bioinformatics program Venny 2.1.0. (bioinfogp.cnb.csic.es/tools/venny/) was used to calculate intersecting DEGs and DEMs.

Gene ontology (GO) and kyoto encyclopedia of genes and genomes (KEGG) enrichment analysis. For all the overlapping DEGs, GO function annotation and KEGG pathway enrichment analyses were conducted using Metascape (version 3.5.20240101, metascape.org/gp/index.html#/main/step1). A significance level of $P<0.01$ was applied. R tool org.Hs.eg.db (version 3.1.0, bioconductor.org/) was used for GO annotation of overlapping DEGs. KEGG pathway gene annotation for overlapping DEGs was obtained using KEGG REST API (version 20230301, kegg.jp/kegg/rest/keggapi.html). Enrichment results were obtained by enrichment analysis using the clusterProfiler R package (version 3.14.3; bioconductor.org/packages/release/bioc/html/clusterProfiler.html). Statistical significance was defined as $P<0.05$ and false discovery rate (FDR)<0.1.

Prediction of miRNA targets. The downstream target genes of overlapping DEMs in the GSE115293 and GSE145305 datasets were predicted using the online bioinformatics tool miRNet (mirnet.ca/miRNet/home.xhtml). The online bioinformatics program Venny 2.1.0 was utilized to identify the intersections between the projected target genes and DEGs. These intersections were used as point-dysregulated target genes for construction of regulatory networks.

miRNA-mRNA network construction and core module analysis. Target gene protein-protein interaction (PPI) files with a highest confidence level >0.9 were acquired from the STRING online database (cn.string-db.org/). To create an interaction network between DEMs and DEGs, the PPI, miRNA and downstream target gene data were combined and imported into the Cytoscape 3.9.1 (cytoscape.org/) for visual analysis. Based on the degree method, the top 10 elements in the network were calculated using the cytoHubba 0.1 (apps.cytoscape.org/apps/cytohubba) plugin for Cytoscape. The component that received the highest score was selected for further research.

Screening of co-expressed genes between HaCaT cell line and psoriatic skin. The raw RNA-sequencing data from the GSE202683 dataset was obtained from GEO database, which contained gene expression levels of four HaCaT cell samples from normal individuals. The sequencing results of these samples in the dataset were compared using the online bioinformatics tool Venny 2.1.0 and the overlapping genes were identified. Using a Venn diagram, the intersection of the HaCaT genes and the DEGs was identified to extract co-expressed genes between the psoriatic skin samples and the HaCaT cell line for further screening.

Prediction of hsa-miR-155-5p targets. miRTarBase 9.0 (mirtarbase.cuhk.edu.cn/~miRTarBase/miRTarBase_2022/php/search.php) and TargetScan 8.0 (targetscan.org/vert_80/) were used to predict the downstream target genes of hsa-miR-155-5p. Venny 2.1.0 was used to obtain the intersection between co-expressed genes of DEGs and HaCaT cells and predicted target genes.

Cell culture. Culture of the immortalized human keratinocyte cell line HaCaT (cat. no. CL-0090; Procell Life Science & Technology Co., Ltd.) was conducted at 37˚C and 5% CO_2 in complete medium, which consisted of 89% MEM, 10% FBS (both Procell Life Science & Technology Co., Ltd.) and 1% penicillium-streptomycin (Wuhan Servicebio Technology Co., Ltd.). The HaCaT cells were authenticated using STR profiling.

Viability of HaCaT cells treated with lipopolysaccharide (LPS). HaCaT cells in the logarithmic growth phase were seeded at a density of $2x10^4$ cells/well in 96-well plates, then cultured at 37˚C with 5% CO_2 overnight. LPS (Sigma-Aldrich; Merck KGaA) was administered at doses of 0.0, 0.1, 0.5, 1.0, 2.0 and 5.0 μg/ml at room temperature. Following 6, 12 and 24 h stimulation, Cell Counting Kit-8 (CCK-8) reagent (Dojindo Laboratories, Inc.) was added to each well. Cells were incubated for a further 2 h at 37˚C in 5% CO_2 and microplate reader was used to measure the absorbance at 450 nm.

Construction of HaCaT cell inflammatory model. An inflammatory model was induced in HaCaT cells by LPS stimulation. HaCaT cells in the logarithmic growth phase were seeded into 6-well plates and incubated overnight at 37˚C with 5% CO_2. Subsequently, the medium was replaced and the cells were stimulated with fresh medium containing 1 μg/ml LPS at 37˚C in 5% CO_2 for 6 h to establish the inflammatory cell model. The aforementioned complete medium was added to the cells for subsequent culture or transfection. Four treatment groups were subsequently established: Negative control (untreated cells), LPS, mimic and LPS + mimic. LPS + mimic group was stimulated with 1 μg/ml LPS for 6 h then transfected with miR-155 mimic.

Cell transfection. miR-155-5p mimic (forward, 5'-UUAAUGCUAAUCGUGAUAGGGGUU-3' and reverse, 5'-CCCCUAUCACGAUUAGCAUUAAUU-3'), mimic negative control (NC; forward, 5'-GCGACGAUCUGCCUAAGAUDTDT-3' and reverse, 5'-AUCUUAGGCAGAUCGUCGCDTDT-3'), miR-155-5p inhibitor (AACCCCUAUCACGAUUAGCAUUAA), inhibitor NC (GUCCCUCACAUCAUAAGCUAAUAA), small interfering (si)-IRF2BP2 (forward, 5'-CUAGUGGAGAGGUCUAUUGTT-3' and reverse, 5'-CAAUAGACCUCUCCACUAGCU-3') and si-NC (forward, 5'-GCGACGAUCUGCCUAAGAUDTDT-3' and reverse, 5'-AUCUUAGGCAGAUCGUCGCDTDT-3') were purchased from Suzhou GenePharma Co., Ltd. For *in vitro* transfection, HaCaT cells were transfected using Lipo8000 (Beyotime Institute of Biotechnology). The concentration of nucleic acid used is 20 μM. Following transfection for 6 h, the culture medium was changed to a complete medium, and the transfected cells continued to be cultured at 37˚C in 5% CO_2 for 48 h for subsequent experiments.

Measurement of cell proliferation. HaCaT cells in the logarithmic growth phase were seeded in 96-well plates and cultivated overnight at 37˚C in an incubator with 5% CO_2. Following transfection, CCK-8 reagent was added to each well and the cells were placed in an incubator with 5% CO_2 at 37˚C. After 2 h, a microplate reader was used to measure the absorbance at 450 nm.

Reverse transcription-quantitative PCR (RT-qPCR). Following the manufacturer's instructions, total RNA was isolated from the transfected cells using TRIzol (Thermo Fisher Scientific, Inc.) and reverse-transcribed. cDNA was synthesized with ReverTra Ace® qPCR RT kit (Toyobo Life Science, Inc.), according to the manufacturer's protocol. qPCR was performed in the CFX Connect real-time system (Bio-Rad Laboratories, Inc.) using SYBR Green qPCR Mix (Monad Biotech Co., Ltd.). The thermocycling conditions were as follows: Initial denaturation at 95˚C for 30 sec; followed by 40 cycles of denaturation at 95˚C for 10 sec, and annealing and extension at 60˚C for 30 sec. U6 and GAPDH were used to standardize the levels of miRNA and gene expression and the $2^{-\Delta\Delta Cq}$ method was employed to calculate the relative expression (24). Table I contains primer sequences that were utilized in the RT-qPCR.

ELISA. A total of $8x10^5$ HaCaT cells/well were seeded into a 6-well plate, then incubated at 37˚C with 5% CO_2 overnight. The cells were induced with LPS for 6 h, as aforementioned. Following transfection, HaCaT cell supernatant was extracted and centrifuged for 20 min at 1,000 x g at 4˚C independently. Levels of IL-1β (cat. no. E-EL-H0149) and IL-6 (cat. no. E-EL-H6156) were determined using ELISA kits (Elabscience Biotechnology, Inc.) following the manufacturer's instructions.

Western blotting (WB). Total protein was extracted from HaCaT cells using RIPA lysis buffer and phosphatase and protease inhibitors (Beyotime Institute of Biotechnology). BCA kit was then used to measure the protein concentration (Wuhan Servicebio Technology Co., Ltd.). Protein (10 μg/lane) were separated using 10% SDS-PAGE, then transferred to PVDF membranes. The membranes were blocked at room temperature for 15 min using rapid blocking solution (Beyotime Institute of Biotechnology), then incubated with primary antibodies overnight at 4˚C. The primary antibodies were as follows: Anti-β-tubulin (cat. no. 10094-1-AP; 1:20,000; Wuhan Sanying Biotechnology), anti-GAPDH

Table I. Primers used in reverse transcription-quantitative PCR.

Primer	Sequence, 5'→3'
hsa-miR-155-5p	F:CCACGGTCTTAATGCTAATCGTGAT
	R: ATCCAGTGCAGGGTCCGAGG
U6	F: AGAGAAGATTAGCATGGCCCCTG
	R: AGTGCAGGGTCCGAGGTATT
IRF2BP2	F: TCCTCTTTTGTGTCTCCGCC
	R: GGCGGACTGTTGCTATTCCT
IL-6	F: TTCGGTCCAGTTGCCTTCTC
	R: CTGAGATGCCGTCGAGGATG
IL-1β	F: AAGTACCTGAGCTCGCCAGT
	R: CTTGCTGTAGTGGTGGTCGG
KLF2	F: CGCTGAGTGAACCCATCCT
	R: CTGTTGAGGTCGTCGTCGG
p65	F: GGCGAGAGGAGCACAGATAC
	R: GCCTCATAGAAGCCATCCCG
GAPDH	F: AATTCCATGGCACCGTCAAG
	R: AGCATCGCCCCACTTGATTT

IRF2BP2, IFN regulatory factor 2 binding protein 2; KLF2, kruppel-like factor 2; F, forward; R, reverse.

(cat. no. GB12002-100; 1:1,500; Wuhan Servicebio Technology Co., Ltd.), anti-IRF2BP2 (cat. no. 18847-1-AP; 1:1,000; Wuhan Sanying Biotechnology), anti-KLF2 (cat. no. A16480; 1:1,000; ABclonal Biotech Co., Ltd.), anti-p65 (cat. no. 10745-1-AP; 1:1,000; Wuhan Sanying Biotechnology) and anti-phosphorylated (p)-p65 (Ser536; cat. no. 3033T; 1:1,000; Cell Signaling Technology, Inc.). HRP-linked goat anti-rabbit (cat. no. A0208; 1:1,000; Beyotime Institute of Biotechnology) or anti-mouse IgG antibody (cat. no. A0216; 1:1,500; Beyotime Institute of Biotechnology) was incubated with the membrane for 1 h at room temperature. BeyoECL Star (Beyotime Institute of Biotechnology) was utilized to visualize the protein bands. ImageJ software (version 1.52a; National Institutes of Health) was used to analyze protein bands.

Immunofluorescence. HaCaT cells were seeded into 24-well plates covered with slides. Following transfection, the cells were fixed for 15 min with 4% paraformaldehyde at room temperature (Wuhan Servicebio Technology Co., Ltd.), permeabilized for 20 min at room temperature using 0.3% Triton-X-100 (Wuhan Servicebio Technology Co., Ltd.), blocked at room temperature for 30 min with 5% BSA (Wuhan Servicebio Technology Co., Ltd.) and incubated overnight with primary antibody (anti-IRF2BP2; cat. no. 18847-1-AP; 1:200; Wuhan Sanying Biotechnology) at 4˚C. The cells were treated with FITC-labeled fluorescent secondary antibody (cat. no. GB22303; 1:2,000; Wuhan Servicebio Technology Co., Ltd.) for 1 h at 37˚C in the dark. DAPI (Wuhan Servicebio Technology Co., Ltd.) was applied to counterstain the nuclei at room temperature for 8 min in the dark, and the slides were blocked at room temperature for 30 sec with a mounting solution containing an anti-fluorescence quenching agent (Wuhan Servicebio Technology Co., Ltd.). Finally, images were collected using a fluorescence microscope (Olympus Corporation).

Cell cycle measurement. HaCaT cells in the logarithmic growth phase were seeded at a density of $8x10^5$ cells/well into 6-well plates and cultured in an incubator with 5% CO_2 overnight at 37˚C. Following transfection, the cells were digested by trypsin at 37˚C for 6 min and centrifuged for 5 min at 200 x g at 4˚C, followed by PBS wash and an overnight fixation in 70% pure ethanol at 4˚C. The supernatant was removed by centrifugation for 5 min at 200 x g at 4˚C, the cells were washed once with PBS then resuspended in propidium iodide for staining at 37˚C for 30 min (Beyotime Institute of Biotechnology). After 30 min light-protected incubation in a water bath at 37˚C, cell cycle measurements were performed using a BD Accuri C6 Plus Flow Cytometer. ModFit LT 5.0 (vsh.com/products/mflt/) was used for analysis.

Dual-luciferase reporter assay. miR-155-5p mimic (forward, 5'-UUAAUGCUAAUCGUGAUAGGGGUU-3' and reverse, 5'-CCCCUAUCACGAUUAGCAUUAAUU-3'), mimic negative control (NC; forward, 5'-GCGACGAUCUGCCUAAGAUDTDT-3' and reverse, 5'-AUCUUAGGCAGAUCGUCGCDTDT-3') were purchased from Suzhou GenePharma Co., Ltd. The binding site between miR-155-5p and IRF2BP2 was predicted by starBase website (rnasysu.com/encori/). The miR-155-5p target sequence on IRF2BP2 was cloned into the pmirGLO vector (Suzhou GenePharma Co., Ltd.), and the dual fluorescein reporter vector IRF2BP2-wild type (WT) or -mutant (MUT) was constructed. 293T cells (cat. no. GNHu17; Cell Bank/Stem Cell Bank, Chinese Academy of Sciences) were cultured at 37˚C and 5% CO_2 in complete medium. 293T cells were co-transfected with miR-155-5p mimic/mimic NC and IRF2BP2-WT/MUT using Lipofectamine 2000 (Invitrogen; Thermo Fisher Scientific, Inc.). Following co-transfection for 6 h, the culture medium was changed to a complete medium, and the transfected cells continued to be cultured at 37˚C in 5% CO_2 for 24 h. luciferase activity was assessed using the dual-luciferase reporter gene assay system (Vazyme Biotech Co., Ltd.) according to the manufacturer's instructions. Firefly luciferase activity was normalized to *Renilla* luciferase activity.

Statistical analysis. All data are presented as the mean ± standard deviation. GraphPad Prism (version 8.0.1; Dotmatics) was used for statistical analyses. Unpaired Student's t test was used to for comparisons between two groups. One-way ANOVA followed by Tukey's post hoc test was used to compare >2 groups. All experiments were repeated three times. $P<0.05$ was considered to indicate a statistically significant difference.

Results

Identification of 660 overlapping DEGs in gene datasets of psoriasis. The raw data from two datasets (GSE166388 and GSE153007) were obtained from the GEO database to identify DEGs associated with psoriasis using GEO2R. There were 2,006 (831 up- and 1,175 downregulated) in the GSE166388 dataset, and 2,259 DEGs (1,116 up- and 1,143 downregulated mRNAs) in the GSE153007 dataset (Fig. 1). In addition, 660

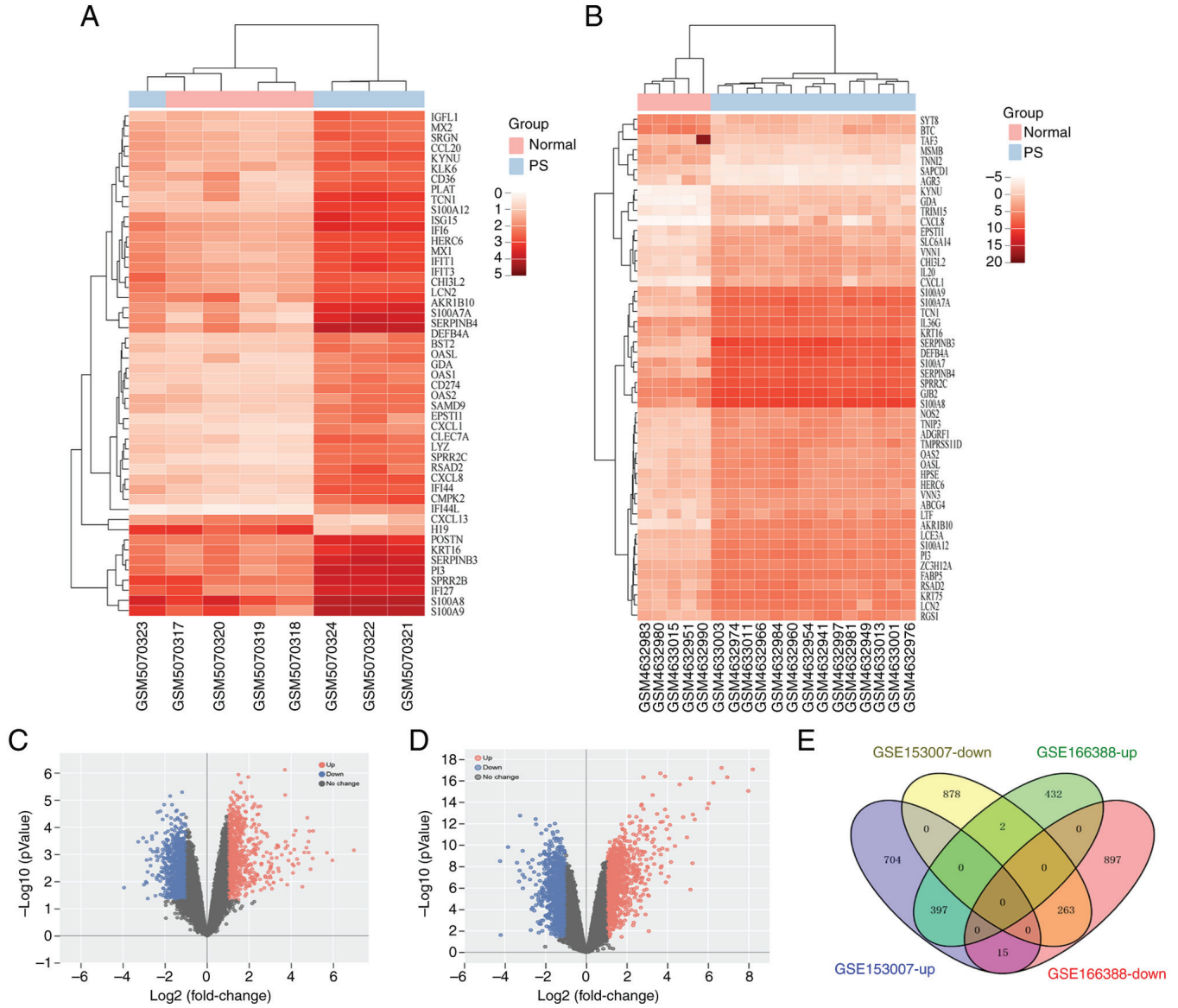

Figure 1. DEGs from GSE166388 and GSE153007 datasets. Heat maps of (A) GSE166388 and (B) GSE153007 DEGs. (C) GSE166388 and (D) GSE153007 DEGs shown as volcano plots. (E) Intersecting DEGs of GSE166388 and GSE153007 datasets. DEG, differentially expressed gene; PS, psoriasis; up, upregulated; down, downregulated.

overlapping DEGs, comprising 263 down- and 397 upregulated mRNAs, were obtained using the online bioinformatics program Venny 2.1.0 (Fig. 1E).

Identification of nine intersecting DEMs in miRNA datasets of psoriasis. The raw data from GSE115293 and GSE145305 were obtained from the GEO database to identify DEMs. The GSE115293 dataset had 177 (66 up- and 111 downregulated), whereas the GSE145305 dataset contained 173 DEMs (106 up- and 67 downregulated; Fig. 2). Additionally, nine intersecting DEMs were identified using Venny 2.1.0. These DEMs included five up- and four downregulated miRNAs (Fig. 2E; Table II).

GO and KEGG enrichment analysis of intersecting DEGs. First, all 660 identified intersecting DEGs were subjected to GO and KEGG analysis using Metascape to investigate their pathways and functions. The top 20 KEGG pathways and GO functional annotation results are shown in Fig. 3A and B. The top 10 KEGG pathways and top 5 GO annotations (including BP, CC and MF) were then applied to 397 overlapping up- and 263 downregulated genes between GSE166388 and GSE153007. According to the results, 'response to biotic stimulus' in BP, 'cytosol' in CC and 'RAGE receptor binding' in MF were the most enriched terms for upregulated genes in the GO analysis (Fig. 4A). 'Measles', 'influenza A' and 'Epstein-Barr virus infection' were the primary enriched pathways in KEGG analysis of the upregulated genes (Figs. 4B and S1). Concurrently, 'response to endogenous stimulus' in BP, 'apical junction complex' in CC and 'transcription coactivator binding' in MF were the most enriched terms for downregulated genes in GO analysis (Fig. 4C). 'Insulin resistance', 'AGE-RAGE signaling in diabetic complications' and 'longevity regulating pathway-multiple species' were the key enriched pathways for downregulated genes in the KEGG enrichment analysis (Figs. 4D and S2).

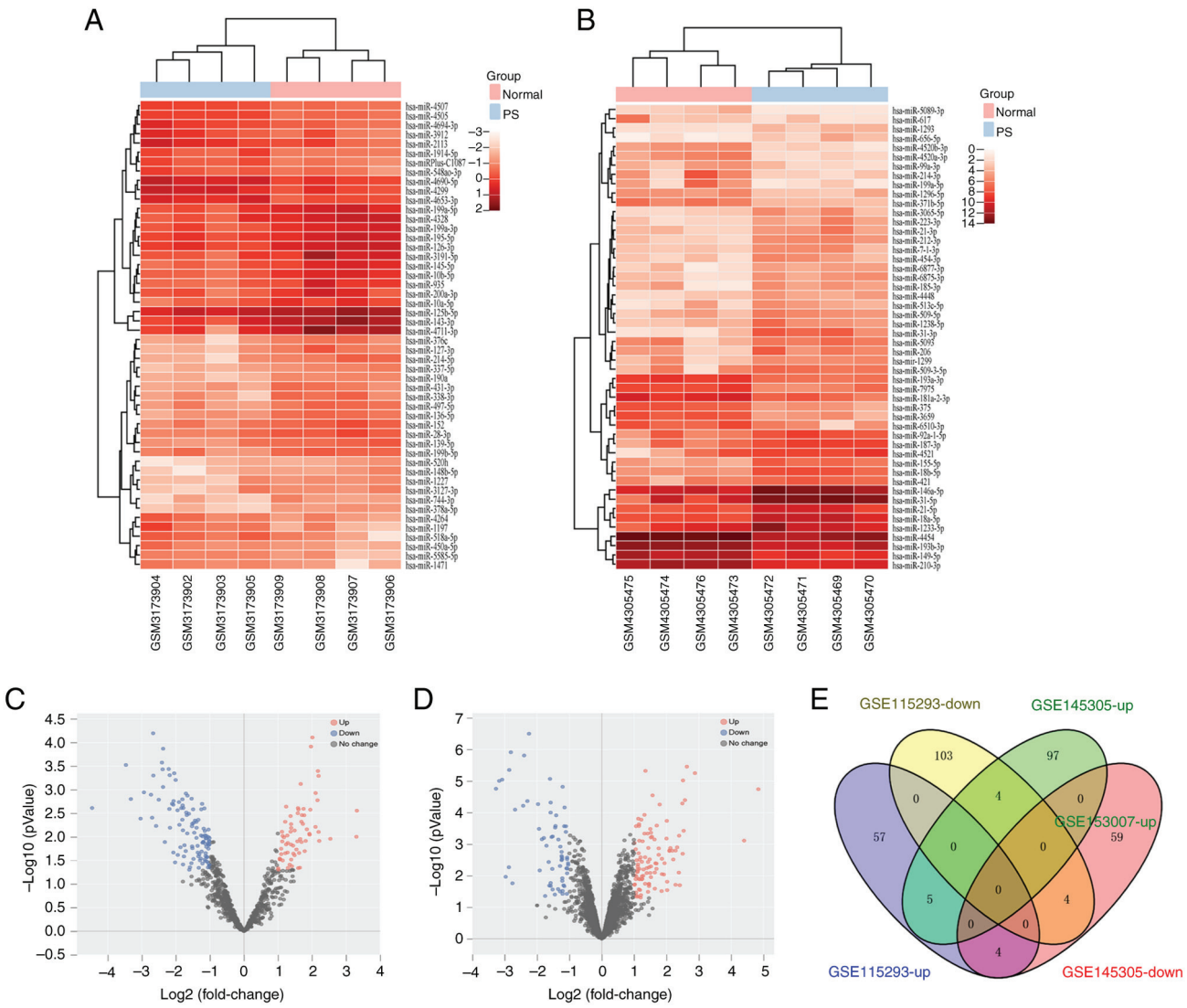

Figure 2. DEMs from GSE115293 and GSE145305 datasets. Heat maps of (A) GSE115293 and (B) GSE145305 DEMs. (C) GSE115293 and (D) GSE145305 DEMs. (E) Intersecting DEMs of GSE115293 and GSE145305 datasets. DEM, differentially expressed microRNA; PS, psoriasis; up, upregulated; down, downregulated.

Table II. Overlapping differentially expressed miRs between GSE115293 and GSE145305.

miR	Regulation
hsa-miR-132-3p	Up
hsa-miR-4725-3p	Up
hsa-miR-25-5p	Up
hsa-miR-155-5p	Up
hsa-miR-378h	Up
hsa-miR-371b-5p	Down
hsa-miR-125b-5p	Down
hsa-miR-497-5p	Down
hsa-miR-199a-5p	Down

miR, microRNA.

Prediction of miRNA targets. Using miRNet, the downstream target genes of nine intersecting DEMs were predicted, yielding 7,232 anticipated target genes. To identify target genes for construction of the miRNA-mRNA network, 660 crossover DEGs and projected miRNA target genes were trimmed simultaneously using Venny 2.1.0 (Fig. 5), resulting in 340 dysregulated crossover target genes.

miRNA-mRNA network construction and core network analysis. PPI data from STRING and miRNA and corresponding downstream target gene data were combined and imported into Cytoscape 3.9.1 to establish an interaction network between psoriasis DEMs and 340 target mRNAs (Fig. 6A). hsa-miR-155-5p was linked with the most target genes, while hsa-miR-4725-3p was linked with the least number of target genes. The degree approach was employed to extract the core network using the cytoHubba plugin in Cytoscape (Fig. 6B). The top 10 elements in psoriasis included six hub genes with elevated expression, including cyclin dependent kinase 1, cyclin A2), CCNB1 (cyclin B1), STAT1, BUB1 mitotic checkpoint serine/threonine kinase) and NCAPG (non-SMC condensin I complex subunit G, as

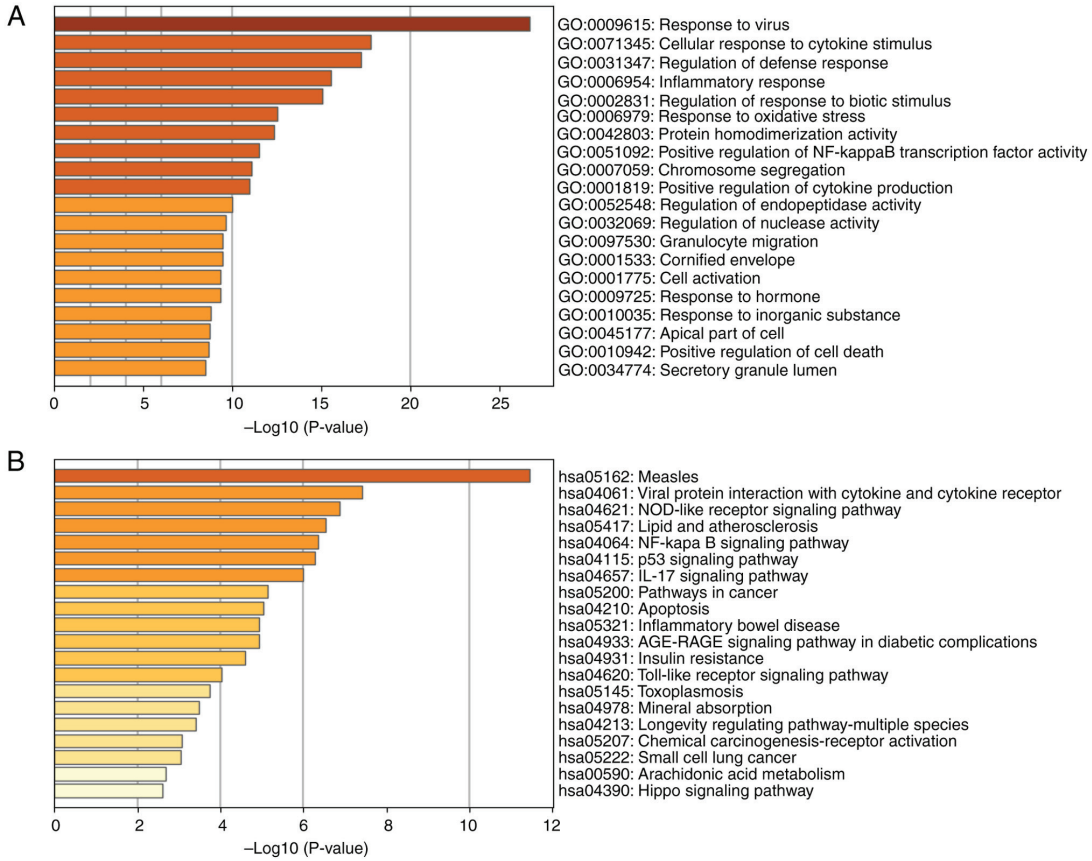

Figure 3. GO and KEGG enrichment of DEGs using Metascape database. Top 20 (A) GO and (B) KEGG analysis results for 660 intersecting DEGs. KEGG, Kyoto Encyclopedia of Genes and Genomes; GO, Gene Ontology; DEG, differentially expressed gene.

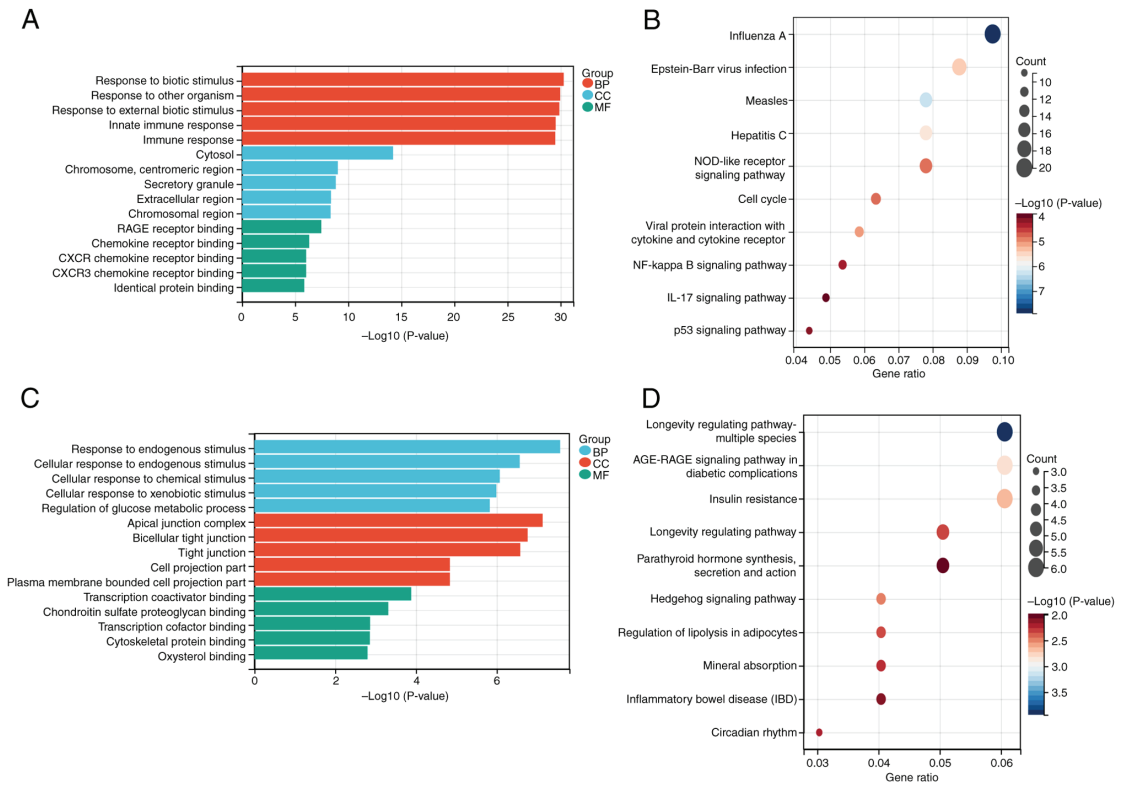

Figure 4. GO and KEGG analysis of up- and downregulated DEGs using R package. (A) Top 5 enrichment terms for upregulated DEGs in the GO annotation. (B) Top 10 enrichment terms for upregulated DEGs in the KEGG pathways. (C) Top 5 enrichment terms for downregulated DEGs in the GO annotation. (D) Top 10 enrichment terms for downregulated DEGs in the KEGG pathways. CC, cellular component; BP, biological process; MF, molecular function; KEGG, Kyoto Encyclopedia of Genes and Genomes; GO, Gene Ontology; DEG, differentially expressed gene.

Table III. Top10 elements of the core network in miRNA-mRNA network construction.

Node	Degree	Regulation
hsa-miR-155-5p	258	Up
hsa-miR-497-5p	70	Down
hsa-miR-132-3p	57	Up
hsa-miR-125b-5p	50	Down
CDK1	31	Up
CCNA2	28	Up
CCNB1	26	Up
STAT1	24	Up
BUB1	23	Up
NCAPG	22	Up

miR, microRNA; CDK1, cyclin-dependent kinase 1; CCNA2, cyclin A2; CCNB1, cyclin B1; BUB1, BUB1 mitotic checkpoint serine/threonine kinase; NCAPG, non-SMC condensin I complex subunit G.

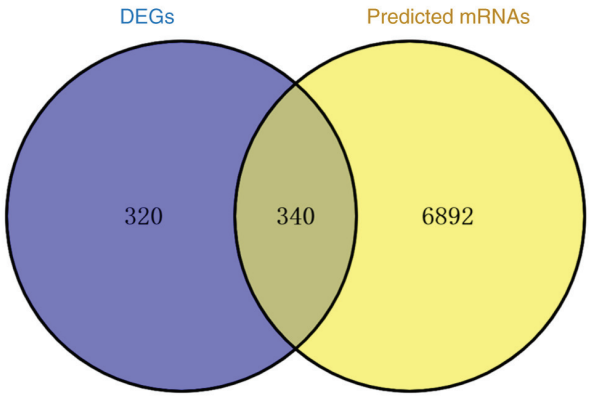

Figure 5. Intersection of 660 DEGs and predicted target genes. DEG, differentially expressed gene.

well as four miRNAs, including upregulated hsa-miR-155-5p and hsa-miR-132-3p and downregulated hsa-miR-497-5p and hsa-miR-125b-5p (Table III). hsa-miR-155-5p, which was upregulated in psoriatic skin, had the highest score and greatest number of associated genes, suggesting it may serve a key role in controlling the onset and progression of psoriasis. Therefore, the function of hsa-miR-155-5p in the control of psoriasis was investigated.

Screening of co-expressed genes between HaCaT cell line and psoriatic skin. The original data from GSE202683 dataset was obtained from the GEO database, which contained gene sequencing results from four HaCaT cell samples. The expression data were analyzed using Venny 2.1.0 to obtain 8,835 overlapping genes that were expressed in HaCaT cells (Fig. 7A). To facilitate screening of target genes, a Venn diagram was used to illustrate the intersect of the 8,835 overlapping genes and 660 significantly DEGs screened in psoriatic skin. From this intersect, 351 co-expressed genes between HaCaT cell line and psoriatic skin were identified (Fig. 7B).

Prediction of hsa-miR-155-5p targets. The downstream target genes of miR-155 were predicted using TargetScan and miRTarBase. In TargetScan database, 556 genes were predicted, whereas 932 genes were predicted in miRTarBase. In addition, intersection of 351 co-expressed genes and predicted target genes was determined using Venny 2.1.0, from which five candidate genes were obtained, including IRF2BP2, claudin 1, CARHSP1 (calcium regulated heat stable protein 1), ARL5B (ADP ribosylation factor like GTPase 5B and TMEM33 (transmembrane protein 33) (Fig. 8). Psoriasis etiology is associated with immunological and inflammatory responses and research has shown that IRF2BP2 is associated with inflammatory responses (12). Therefore, IRF2BP2 was selected for further investigation.

Impact of LPS on HaCaT cell viability. The viability of HaCaT cells treated with LPS was assessed using CCK-8 reagent (Fig. 9). Compared with 0.0 μg/ml LPS, HaCaT cell viability increased after 6 and 12 h of LPS stimulation but decreased after 24 h. After 6 and 12 h of LPS stimulation, the cell viability of HaCaT cells changed significantly when the concentration of LPS was 0.0-0.5 μg/ml and 2-5 μg/ml. The viability of HaCaT cells was the highest after LPS stimulation for 6 h. Since the change of LPS concentration has a great influence on the viability of HaCaT cells, and when the LPS stimulation concentration is ~1 μg/ml, the viability of HaCaT cells is relatively stable. Therefore, treatment with 1 μg/ml LPS for 6 h was selected for subsequent experiments.

Proliferation of HaCaT cells is inhibited by miR-155-5p overexpression. HaCaT cells were transfected with miR-155 mimic and NC to evaluate the effect of miR-155 on the biological function of cells. miR-155 mimic significantly enhanced expression of miR-155 (Fig. 10A). HaCaT cell proliferation was assessed using CCK-8 reagent 48 h after transfection. miR-155 mimic significantly suppressed HaCaT cell proliferation compared with control and mimic NC group (Fig. 10B). Overexpressing miR-155 may prevent proliferation of HaCaT cells.

Overexpression of miR-155-5p arrests cells in S phase. Following transfection with the miR-155 mimic and corresponding mimic NC, flow cytometry was conducted. miR-155 mimic group had significantly fewer cells in G1 and G2 phases and significantly more cells in S phase compared with the control and mimic NC groups. However, there was no significant difference in the cell cycle distribution between the control and mimic NC groups (Fig. 11). Overexpression of miR-155 promoted cells from G1 phase into S phase and arrested cells in the S phase, thus significantly the number of cells in S phase.

miR-155 and pro-inflammatory cytokines are expressed at higher levels following LPS stimulation. RT-qPCR results showed that miR-155 expression was significantly higher following LPS stimulation compared with untreated control (Fig. 12A). Similarly, levels of IL-1β and IL-6 inflammatory cytokines were also higher (Fig. 12B and C). ELISA demonstrated IL-1β and IL-6 levels were significantly elevated following LPS stimulation (Fig. 12D and E). These results suggested that LPS promoted the secretion of inflammatory

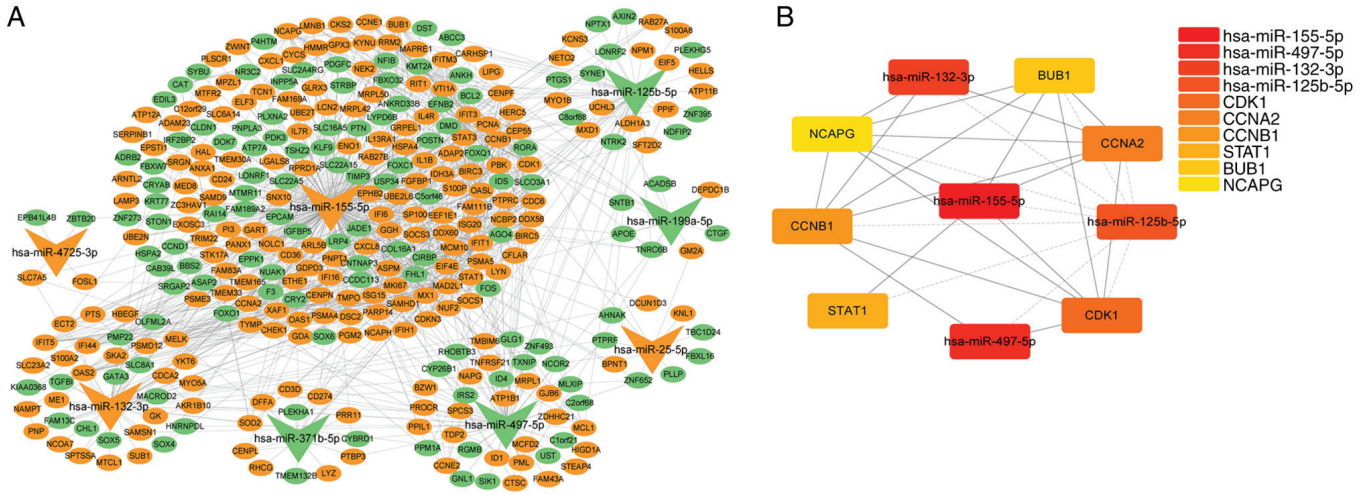

Figure 6. miRNA-mRNA network and key modules. (A) miRNA-mRNA regulatory network. Orange, upregulation; green, downregulation; triangle, miRNA; ellipse, mRNA. (B) Core network was retrieved using the cytoHubba plug-in. The red icon has the highest score, followed by the orange icon and the yellow icon has the lowest score. miRNA, microRNA.

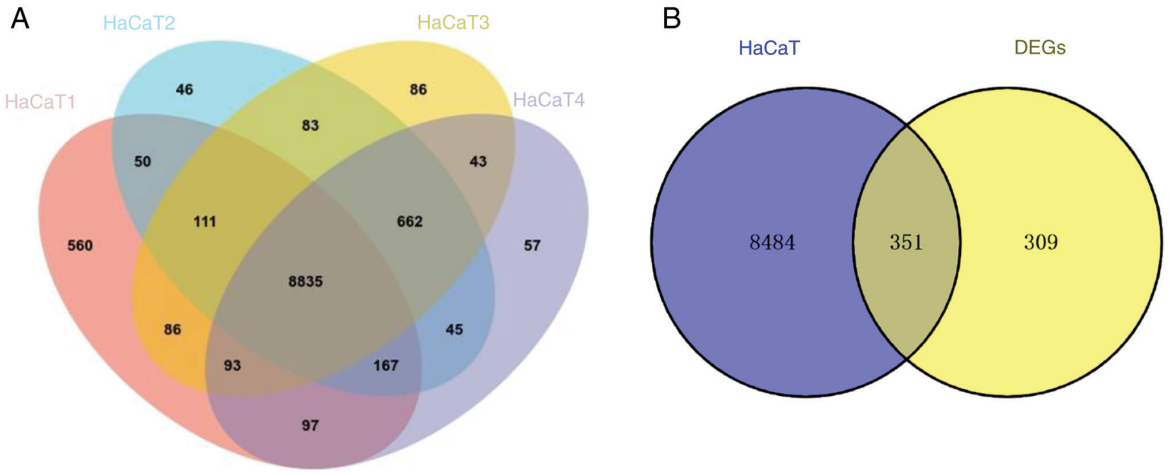

Figure 7. Co-expressed genes between HaCaT cell line and psoriatic skin. (A) Co-expressed genes in four HaCaT cell samples in the GSE202683 dataset. (B) Intersection of 8,835 co-expressed genes and 660 DEGs. DEG, differentially expressed gene.

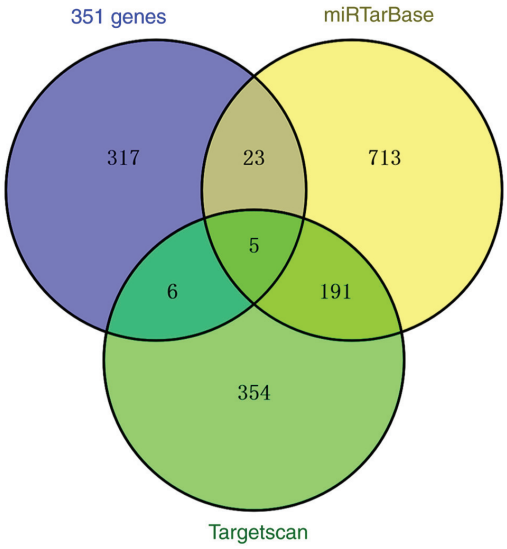

Figure 8. Intersection of 351 co-expressed genes and predicted target genes of miR-155-5p. miR, microRNA.

factors by HaCaT cells. LPS was successfully used to establish an *in vitro* inflammatory cell model. In line with the aforementioned bioinformatics study, levels of miR-155 were raised during *in vitro* inflammatory stimulation.

Overexpression of miR-155 enhances inflammatory response of HaCaT cells following LPS stimulation. RT-qPCR results demonstrated that overexpression of miR-155 significantly increased expression of miR-155 and inflammatory response, as indicated by the increased IL-1β and IL-6 levels compared with NC group (Fig. 13A-C). ELISA showed that the concentrations of IL-1β and IL-6 secreted by HaCaT cells stimulated with LPS were significantly enhanced by sustained overexpression of miR-155 (Fig. 13D and E). These findings verified that overexpression of miR-155 increased the response to inflammation in HaCaT cells.

Inflammatory response induced by LPS stimulation in HaCaT cells is suppressed by silencing miR-155. RT-qPCR

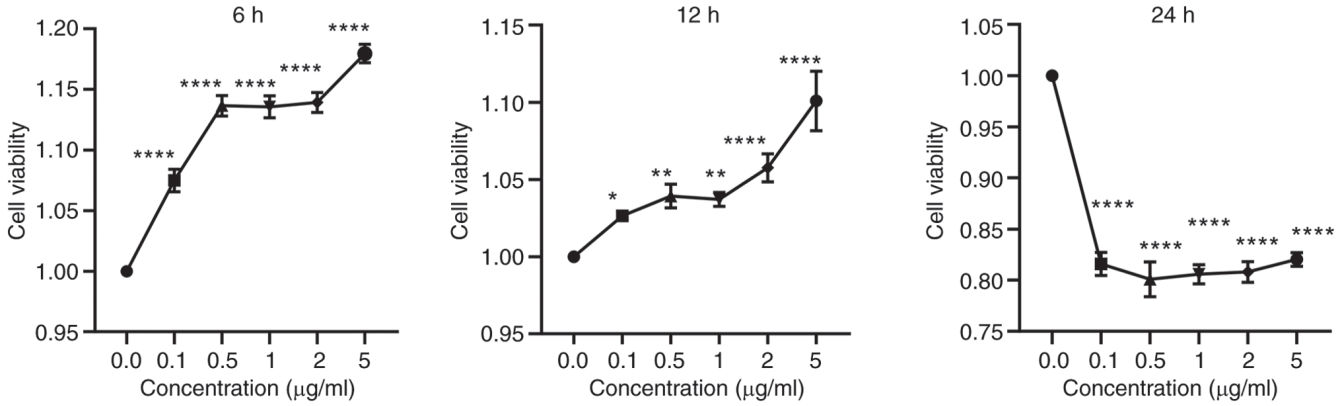

Figure 9. Effect of LPS on the viability of HaCaT cells. LPS, lipopolysaccharide. *P<0.05, **P<0.01, ****P<0.0001.

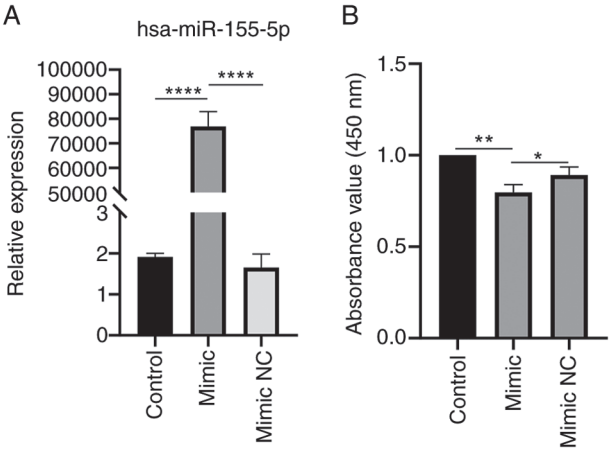

Figure 10. Effect of miR-155 on HaCaT cell proliferation. (A) Transfection efficiency of miR-155 mimic. (B) Cell proliferation was detected by Cell Counting Kit-8 reagent. *P<0.05, **P<0.01, ****P<0.0001. miR, microRNA; NC, negative control.

demonstrated that suppressing miR-155 expression during LPS stimulation significantly decreased miR-155 expression levels compared with NC (Fig. 14A). Silencing miR-155 expression significantly reduced the expression of IL-1β and IL-6 (Fig. 14B-E). Taken together, these findings indicated a significant decrease in the inflammatory response of HaCaT cells under inflammatory conditions when miR-155-5p was silenced.

miR-155-5p interacts with IRF2BP2 to negatively regulate IRF2BP2 expression. starBase was used to predict binding sites between miR-155-5p and IRF2BP2 (Fig. 15A). Dual-luciferase reporter assay was used to verify whether miR-155-5p targeted IRF2BP2. miR-155-5p mimic significantly inhibited luciferase activity of IRF2BP2-WT in 293T cells, while luciferase activity of IRF2BP2-MUT and pmirGLO groups did not change (Fig. 15B). HaCaT cells were transfected with miR-155-5p mimic/mimic NC or miR-155-5p inhibitor/inhibitor NC to determine the association between miR-155-5p and IRF2BP2. The expression of miR-155-5p was significantly elevated following transfection with miR-155 mimic and significantly decreased upon transfection with miR-155 inhibitor (Fig. 15C). The RT-qPCR showed that, compared with the NC group, the IRF2BP2 gene expression was decreased upon transfection with miR-155 mimic and increased by miR-155 inhibitor (Fig. 15D). The results of the WB experiments confirmed overexpression of miR-155 reduced IRF2BP2 protein expression and miR-155 silencing promoted IRF2BP2 protein expression (Fig. 15E). Overexpression of miR-155 decreased nuclear expression of IRF2BP2 protein, and inhibition of miR-155 enhanced the nuclear expression of IRF2BP2 protein (Fig. 15F) suggesting miR-155-5p decreased IRF2BP2 expression and that IRF2BP2 was a target gene of miR-155-5p.

Suppression of inflammatory cytokine expression by miR-155-5p inhibitor is reversed by knockdown of IRF2BP2. Knockdown efficiency of si-IRF2BP2 is shown in Fig. S3. RT-qPCR and ELISA showed that under LPS stimulation, the gene expression and protein secretion of IL-1β and IL-6 were significantly decreased in the miR-155 inhibitor group compared with inhibitor NC group (Fig. 16A and B). Under LPS stimulation, gene expression and protein secretion levels of IL-1β and IL-6 in miR-155 inhibitor + si-IRF2BP2 group were significantly increased compared with miR-155 inhibitor group (Fig. 16A and B). miR-155 inhibitor increased expression of IRF2BP2 gene and protein under LPS stimulation (Fig. 16C and D). However, expression levels of IRF2BP2 gene and protein were significantly decreased in the miR-155 inhibitor + si-IRF2BP2 compared with the miR-155 inhibitor group. Collectively, these results suggested that inhibition of inflammatory cytokine expression by miR-155-5p inhibitor was reversed by knockdown of IRF2BP2 and miR-155-5p regulated inflammation in HaCaT cells by targeting IRF2BP2.

miR-155 may promote inflammatory response of HaCaT cells via the IRF2BP2/KLF2/NF-κB pathway. To examine the molecular mechanism underlying how miR-155 targets IRF2BP2 to promote inflammation in HaCaT cells, an inflammation model was induced by stimulating cells with 1 μg/ml LPS for 6 h. Gene expression levels of IRF2BP2, KLF2 and p65 were determined by RT-qPCR and protein expression levels of IRF2BP2, KLF2, p65 and p-p65 were determined by WB. Following LPS stimulation, gene expression levels of IRF2BP2 and KLF2 were decreased, while the expression of p65 was increased compared with the control group (Fig. 17A). RT-qPCR (Fig. 17B) and WB (Fig. 17C-E) results confirmed

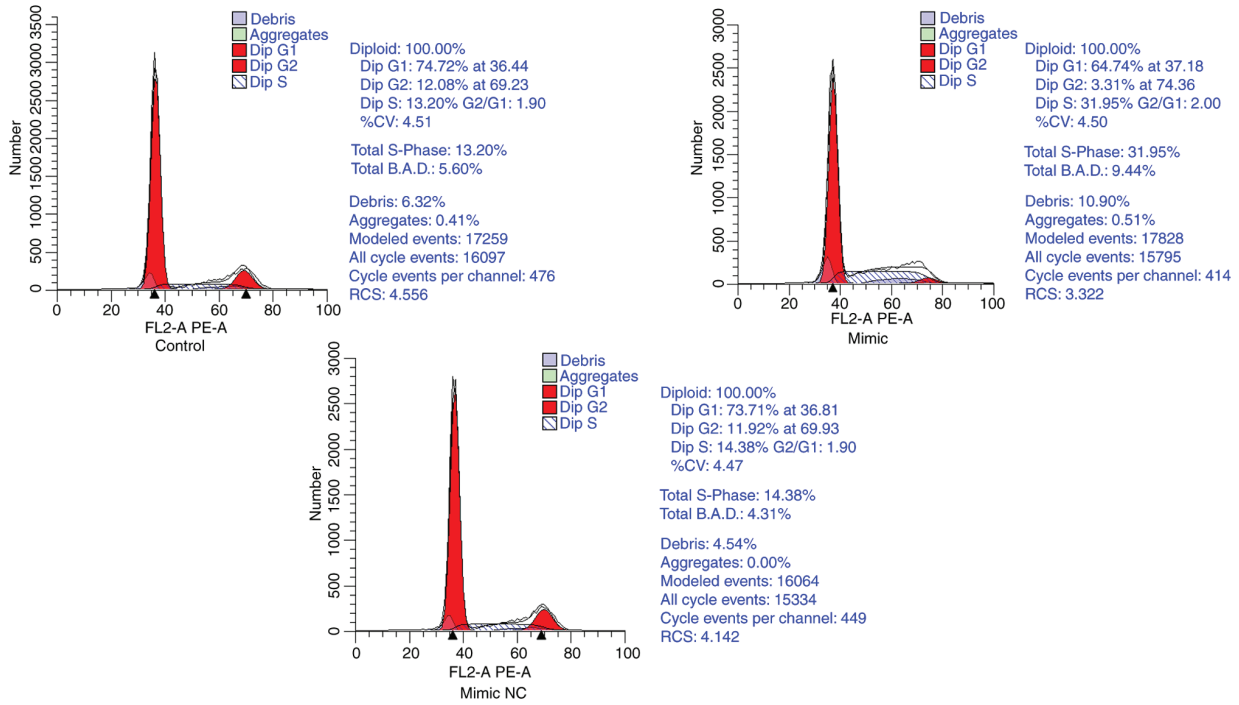

Figure 11. Effect of microRNA-155 on HaCaT cell cycle progression. Dip, diploid; CV, coefficient of variation; BAD, background aggregates and debris; RCS, reduced χ-square; NC, negative control.

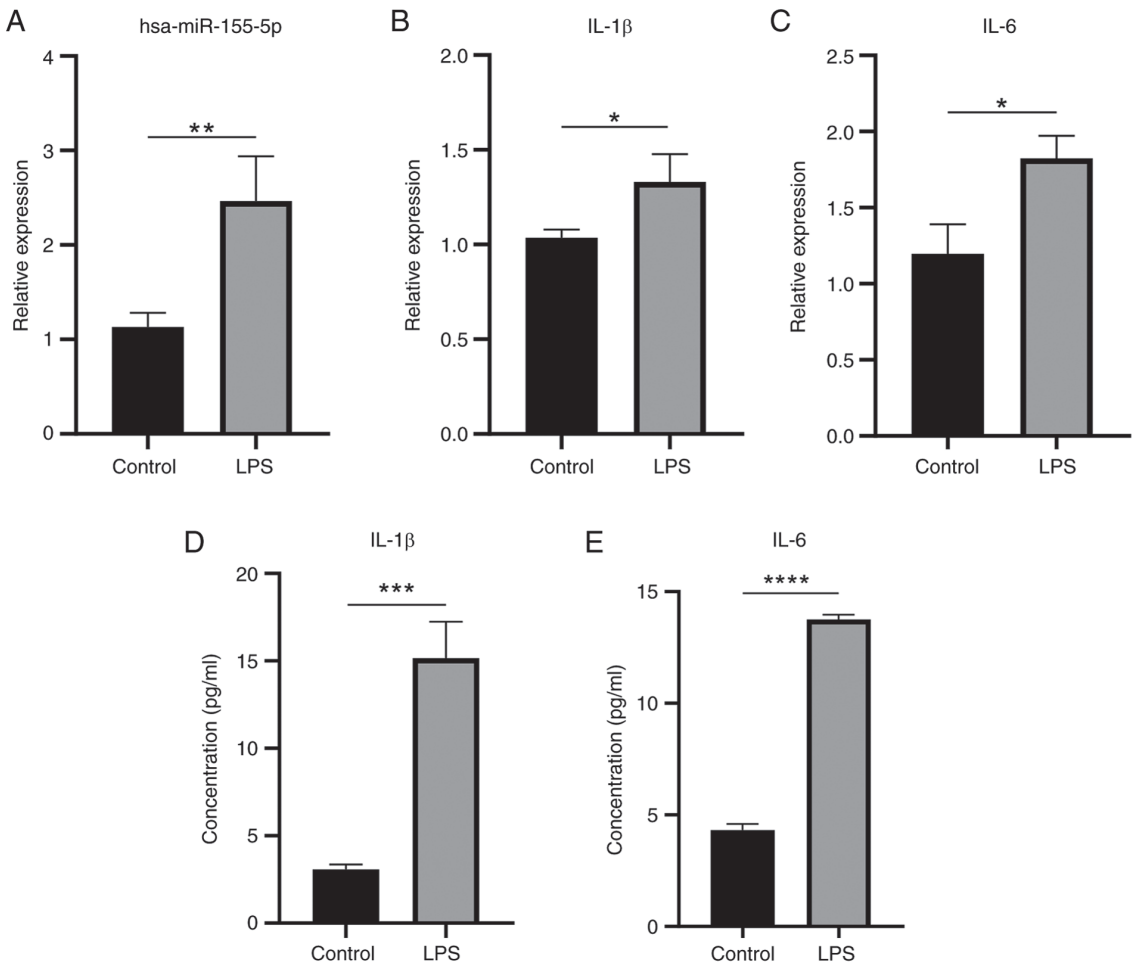

Figure 12. Effect of LPS on miR-155, IL-1β and IL-6 expression and cytokine production. Reverse transcription-quantitative PCR was used to ascertain expression levels of (A) miR-155, (B) IL-1β and (C) IL-6 in LPS-stimulated HaCaT cells. ELISA was used to quantify levels of (D) IL-1β and (E) IL-6 in the culture media of HaCaT cells. *P<0.05, **P<0.01, ***P<0.001, ****P<0.0001. LPS, lipopolysaccharide; miR, microRNA.

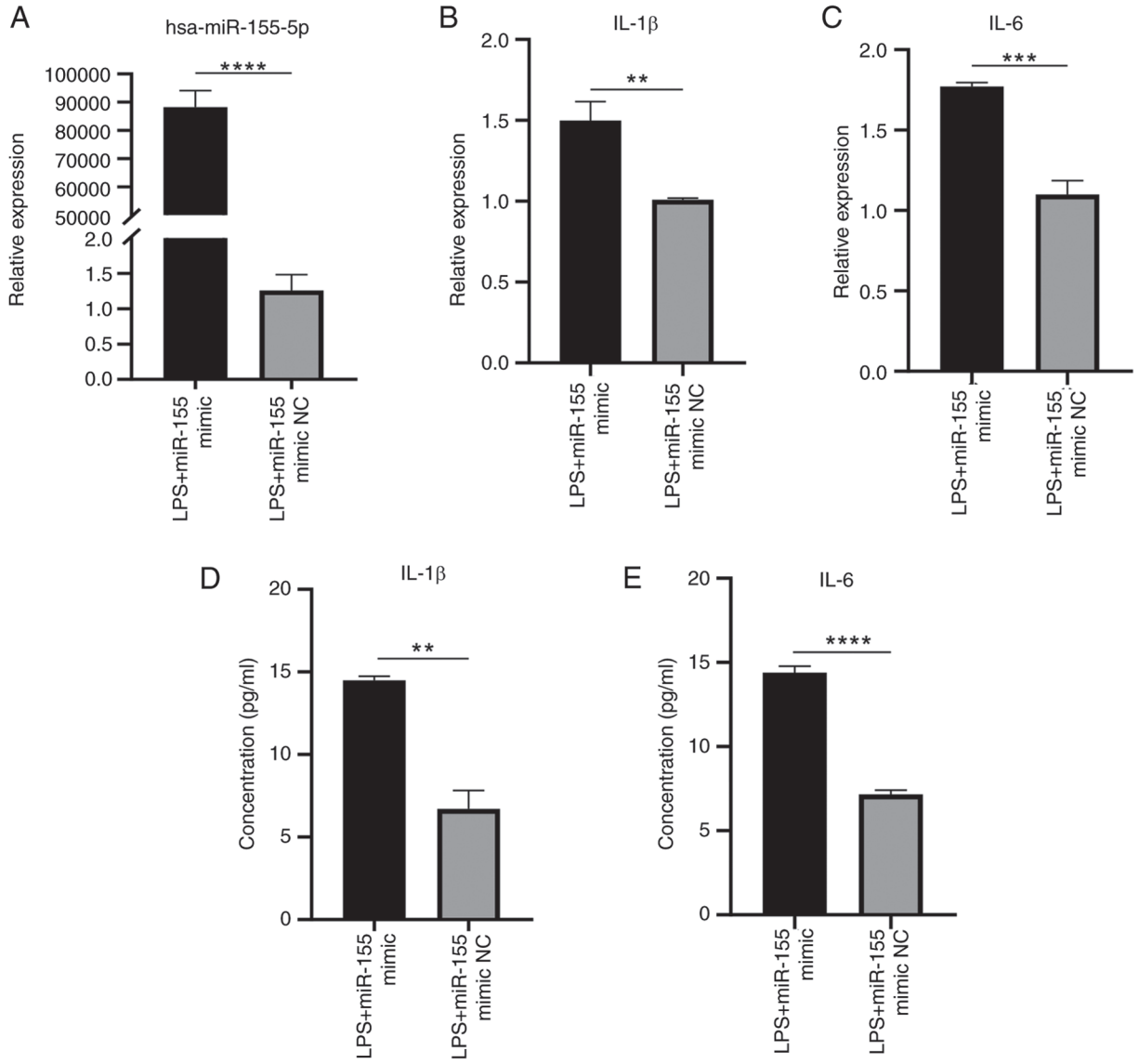

Figure 13. Expression of miR-155, IL-6 and IL-1β and cytokine secretion following overexpression of miR-155 and LPS stimulation. Reverse transcription-quantitative PCR was used to assess (A) miR-155, (B) IL-1β and (C) IL-6 gene expression. ELISA was applied to measure levels of (D) IL-1β and (E) IL-6 in the culture media of HaCaT cells. **P<0.01, ***P<0.001, ****P<0.0001. LPS, lipopolysaccharide; miR, microRNA; NC, negative control.

that the IRF2BP2 expression was significantly reduced in the LPS, mimic and LPS + mimic groups compared with the control. Similarly, KLF2 expression was suppressed. However, compared with the control group, p-p65 protein expression was higher in the LPS, mimic and LPS + mimic groups. In summary, under inflammatory conditions, overexpression of miR-155 inhibited IRF2BP2 and decreased KLF2 expression. p-p65 protein expression increased and secretion of inflammatory factors IL-1β and IL-6 were enhanced, thereby promoting the inflammatory response of HaCaT cells.

Discussion

Psoriasis is a chronic and recurrent inflammatory skin condition with a complicated pathophysiology. The molecular processes underlying the onset and recurrence of this illness may be impacted by numerous variables, including immunological, genetic and environmental factors. According to a previous study, skin barrier malfunction and clinical psoriasis may result from interaction between immune cells and epidermal keratinocytes, which may stimulate signaling pathways, promote production of inflammatory chemokines and cytokines and induce aberrant differentiation and overproliferation of epidermal keratinocytes (25). Further study of the molecular mechanisms underlying proliferation and aberrant differentiation of epidermal keratinocytes may therefore promote understanding of the pathogenesis of psoriasis (26).

Small non-coding RNAs known as miRNAs are key for controlling post-transcriptional gene expression. To control translational suppression or degradation, miRNAs bind in entire or partial complementation to the 3'-untranslated region of mRNAs that code for proteins (27,28). miRNAs control keratinocyte differentiation, proliferation, apoptosis and inflammation and activation of T cell subsets, in addition to serving numerous roles in inflammatory skin disorders (29,30). A previous study observed notable upregulation of miR-155, miR-146a and miR-21 in skin lesions from patients with psoriasis (31). The pathogenesis of psoriasis is

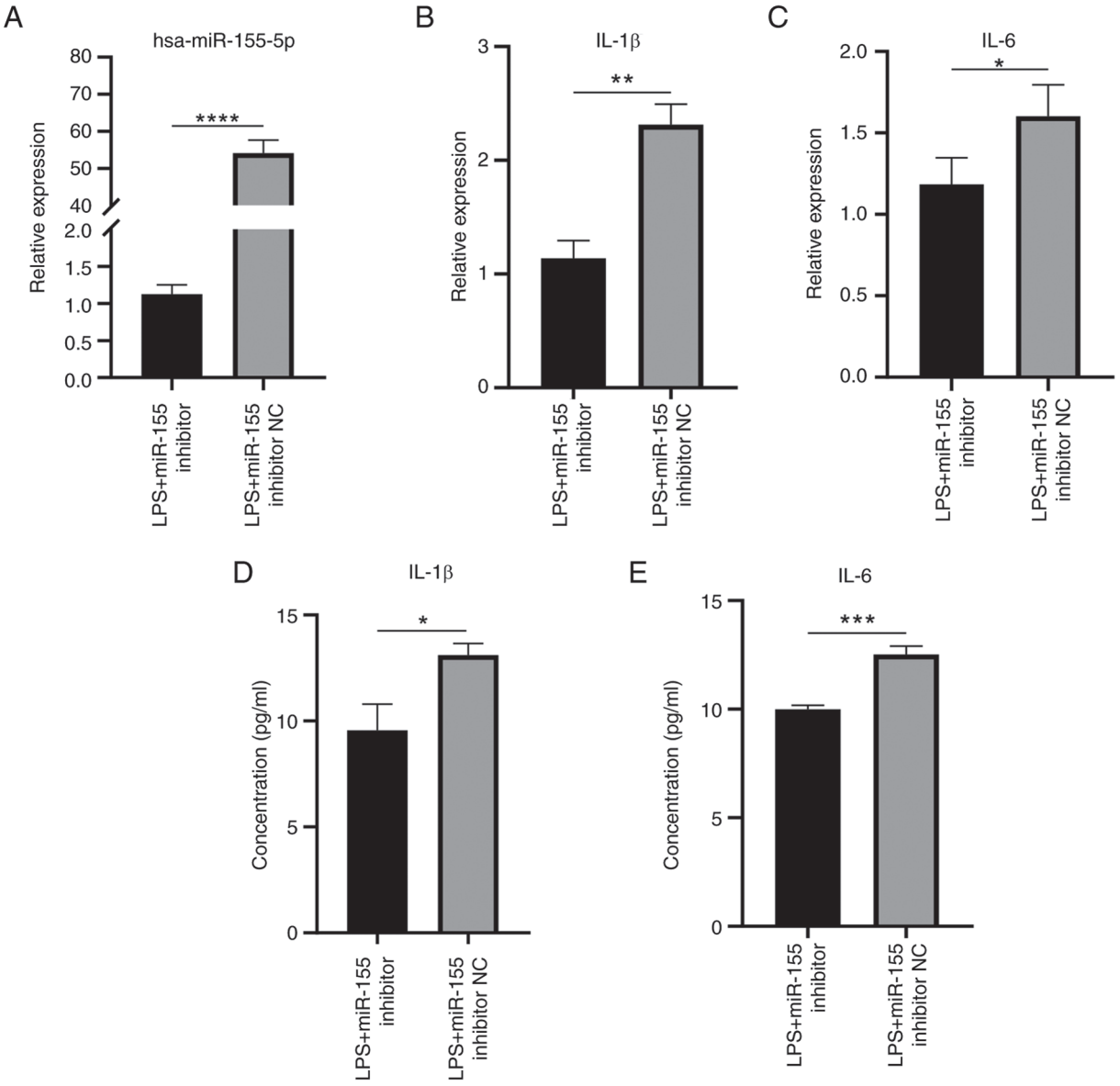

Figure 14. Expression of miR-155, IL-16 and IL-1β and cytokine secretion following inhibition of miR-155 and LPS stimulation. Reverse transcription-quantitative PCR was used to ascertained (A) miR-155, (B) IL-1β and (C) IL-6 gene expression levels. ELISA was performed to measure the levels of (D) IL-1β and (E) IL-6 in the culture media of HaCaT cells. *P<0.05, **P<0.01, ***P<0.001, ****P<0.0001. LPS, lipopolysaccharide; miR, microRNA; NC, negative control.

associated with dysregulation of miRNA expression and regulatory targets, which may be useful indicators for diagnosis, monitoring disease progression and assessing efficacy of treatment (32,33). Therefore, understanding miRNA-mediated regulatory mechanisms of psoriasis offers opportunity to uncover the pathogenesis and improve the treatment strategy for this condition.

In psoriasis, upregulation of miR-155 reduces loricrin levels in keratinocytes, which alters the functions of the epidermal barrier (9). In addition, toll-like receptor 4 activation enhances the inflammatory response triggered by miR-155 in an *in vitro* keratinocyte model (34). miR-155 also promotes cell proliferation and inhibits apoptosis in psoriasis via the PTEN signaling pathway (11). Furthermore, by targeting tumor protein p53 inducible nuclear protein 1, miR-155 increases glycolysis in psoriatic mesenchymal stem cells. Compared with normal human bone marrow mesenchymal stem cells, psoriatic mesenchymal stem cells showed significantly higher glycolysis levels and dysregulated glucose metabolism, highlighting its role in metabolic problems associated with psoriasis (35). In the pathophysiology of psoriasis, the production and release of proinflammatory cytokines such as TNF-α, IFN-γ, and IL-1β are increased (1). Wang *et al* (36) showed that miR-155 affects development of psoriasis by regulating the GATA binding protein 3)/IL37 axis, which regulates the production of proinflammatory cytokines IL-6 and C-X-C motif chemokine ligand 8 in response to TNF-α activation. Additionally, tissue with psoriatic lesions exhibits a notable increase in miR-155 expression (36). Beer *et al* (9) discovered that proinflammatory cytokines IL-17, INF-γ and IL-1β effectively increase miR-155 expression in keratinocytes *in vitro*. These findings align with the present upregulation of miR-155 expression and promotion of inflammatory factor production after establishing an *in vitro* inflammatory model with LPS.

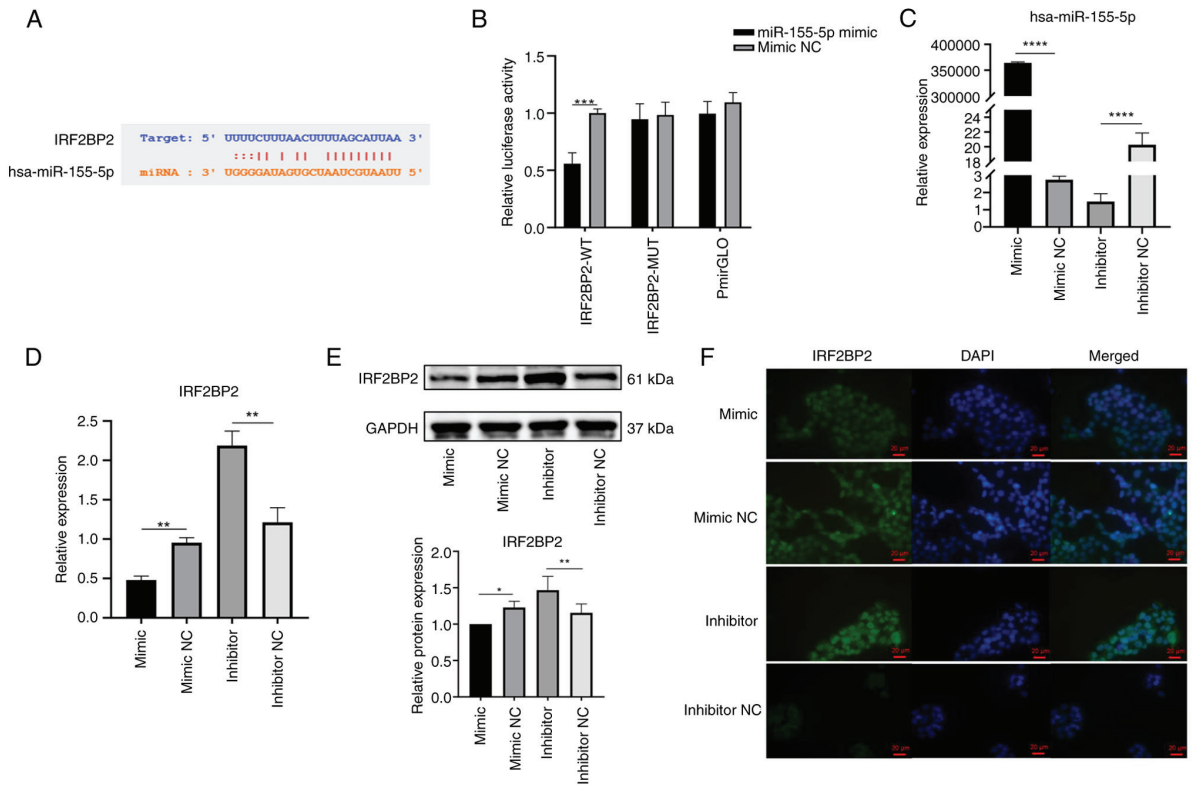

Figure 15. Effect of miR-155 on target gene IRF2BP2. (A) starBase database was used to predict binding sites between miR-155-5p and IRF2BP2. (B) Dual-luciferase reporter assay was used to validate the interaction between miR-155-5p and IRF2BP2. (C) Transfection efficiency of miR-155 was measured by reverse transcription-quantitative PCR. (D) Reverse transcription-quantitative PCR was used to measure the IRF2BP2 mRNA expression. (E) Western blotting was utilized to determine the relative IRF2BP2 protein expression. (F) Localization and relative expression of IRF2BP2 protein were detected by immunofluorescence. *P<0.05, **P<0.01, ***P<0.001, ****P<0.0001. miR, microRNA; IRF2BP2, IFN regulatory factor 2 binding protein 2; NC, negative control; WT, wild-type; MUT, mutant.

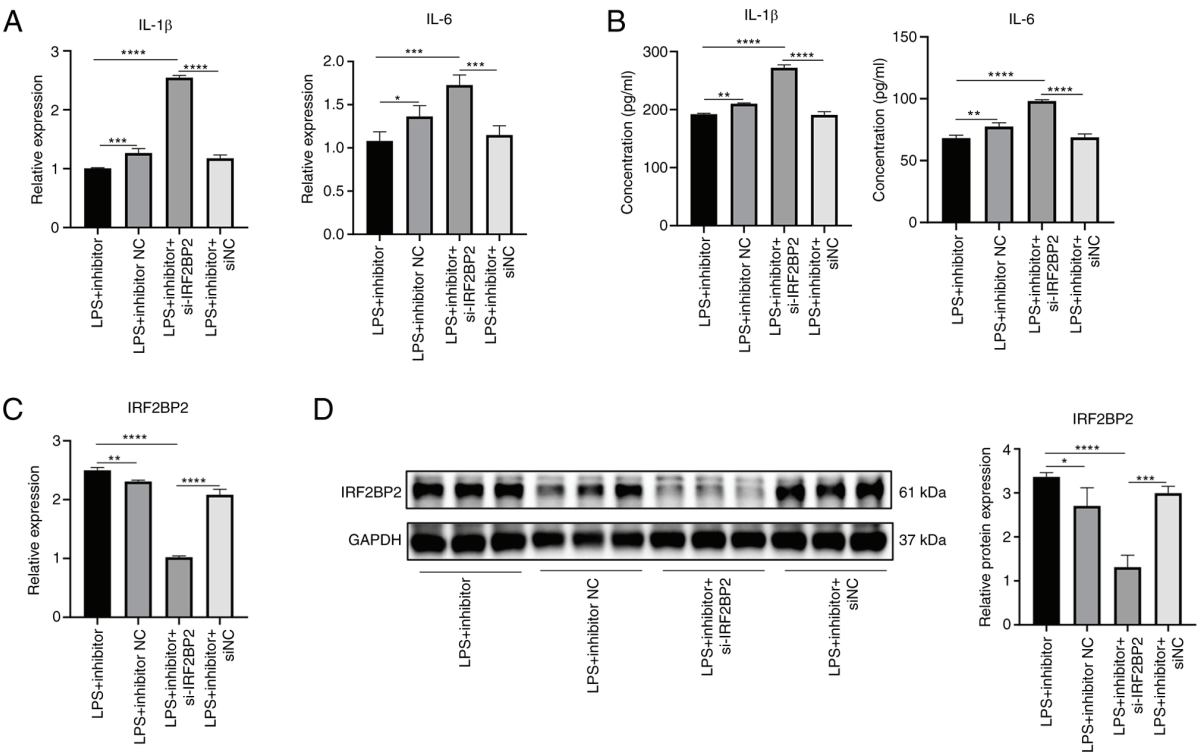

Figure 16. Inhibition of inflammatory cytokine expression by miR-155-5p inhibitor is reversed by knockdown of IRF2BP2. (A) RT-qPCR was used to determine gene expression of IL-1β and IL-6 inflammatory cytokines. (B) Levels of IL-1β and IL-6 in HaCaT cell culture medium were determined by ELISA. (C) IRF2BP2 gene expression was detected by RT-qPCR. (D) IRF2BP2 protein expression was detected by western blotting. *P<0.05, **P<0.01, ***P<0.001, ****P<0.0001. RT-q, reverse transcription-quantitative; miR, microRNA; IRF2BP2, IFN regulatory factor 2 binding protein 2; NC, negative control; si, small interfering.

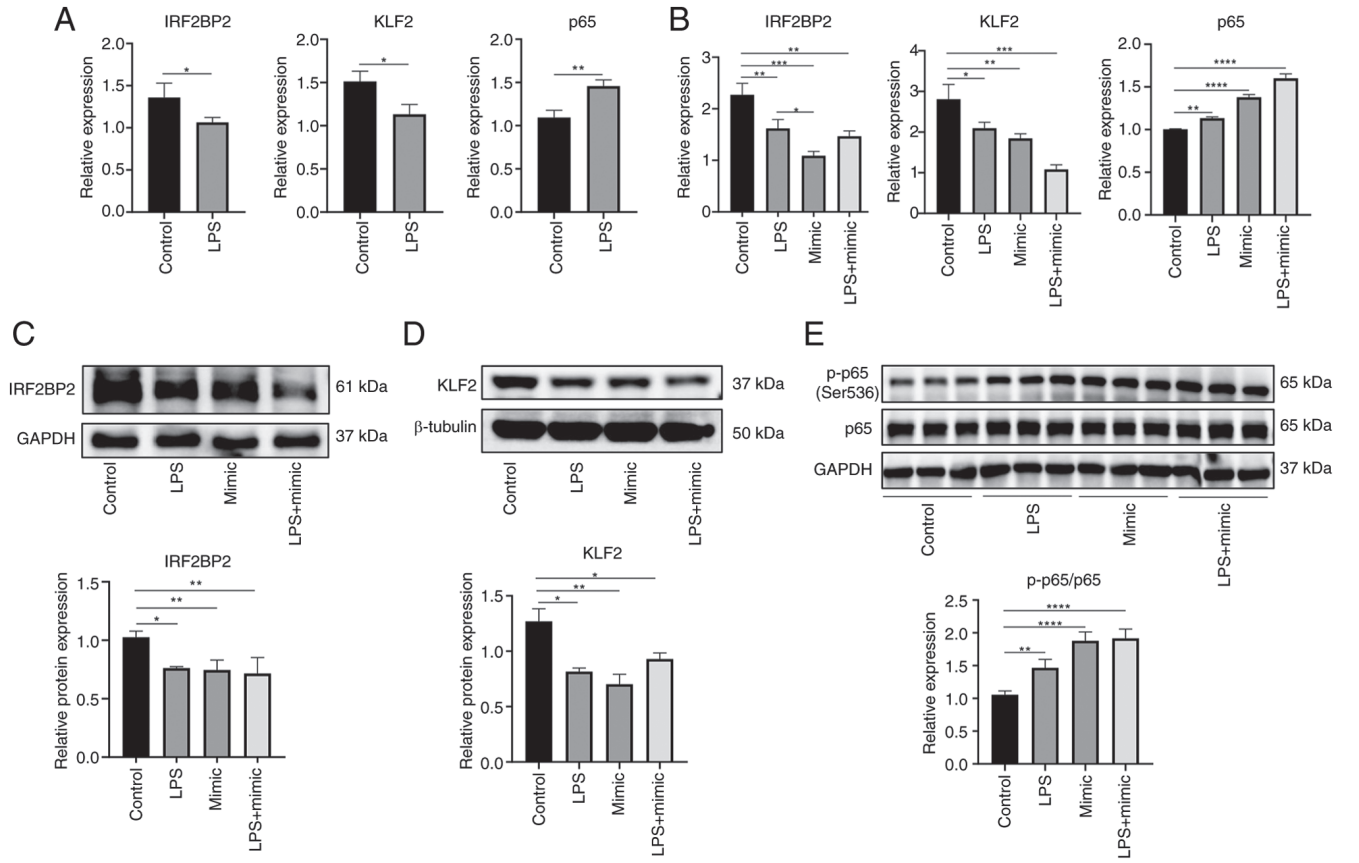

Figure 17. Effect of miR-155 on IRF2BP2, KLF2 and p65 following LPS stimulation. mRNA expression of IRF2BP2, KLF2 and p65 following (A) LPS stimulation and (B) transfection was determined by reverse transcription-quantitative PCR. Relative protein expression levels of (C) IRF2BP2, (D) KLF2 and (E) p65/p-p65 were measured by western blotting. *P<0.05, **P<0.01, ***P<0.001, ****P<0.0001. LPS, lipopolysaccharide; miR, microRNA; IRF2BP2, IFN regulatory factor 2 binding protein 2; p-, phosphorylated; KLF2, kruppel-like factor 2; NC, negative control.

According to Xu *et al* (11), miR-155 affects progression of the cell cycle in HaCaT cells by controlling genes that are part of the signaling pathway associated with cyclin, which causes the cell cycle to move from G1 to the S phase. IRF2BP2 has an important role in both cell cycle regulation and proliferation: Koeppel *et al* (37) demonstrated that overexpression of IRF2BP2 increased the number of cells in S phase and decreasing the number of cells in G2 phase. The present study demonstrated that overexpression of miR-155 in HaCaT cells significantly impacted cell cycle progression, causing most cells to transition from G1 to the S phase and preventing entry into the G2 phase, resulting in a notable increase in S phase cells. These results aligned with those previously reported (11,37). The present study also verified that miR-155 directly targeted IRF2BP2 expression.

NF-κB controls production of growth genes and the immunological response and is found in the cytoplasm. NF-κB is associated with several physiological and pathological processes as it is essential in cell proliferation, inflammation and carcinogenesis (38,39). Following activation of the NF-κB pathway, p-IκBα is activated and degraded and the p65/p50 complex is activated by post-translational modification and transported to the nucleus to participate in transcriptional regulation of downstream target genes (38). A previous study demonstrated that LPS stimulation induces the activation and signaling of the NF-κB (p65/p50) proinflammatory transcription factor complex, thereby promoting expression of p65/p50 and subsequently upregulating miR-146a and miR-155 (40). In line with previous research (40), the present study demonstrated that both LPS stimulation and miR-155 overexpression significantly increased levels of p-p65 protein at ser536. Increased phosphorylation of the p65 subunit led to activation of the NF-κB pathway.

Using chromatin immunoprecipitation and luciferase reporter assay, a previous study discovered that IRF2BP2 binds KLF2 promoter and promotes KLF2 expression in a myocyte enhancer factor 2C-dependent manner (16). As members of the zinc finger family of DNA-binding transcription factors, KLFs are key for a number of biological processes, including inflammation, differentiation and proliferation (41). In addition to serving as a key regulator in certain aberrant and pathological conditions such as rheumatoid arthritis, atherosclerosis and bacterial infection, KLF2 also regulates immune cell activity and function (42-45). Patients experiencing either acute or chronic inflammation exhibit a 30-50% decrease in KLF2 expression (46,47). In the present study, decreased expression of KLF2 was confirmed by RT-qPCR and WB, consistent with the literature (46,47). According to some studies (46,48), KLF2 mediates inhibition of the activity of pro-inflammatory NF-κB, thereby inhibiting the inflammatory response. To inhibit transcriptional activity of the NF-κB proinflammatory signal, KLF2 is recruited to the p300/cAMP response element-binding protein-associated factor. This results in a decrease in production of numerous

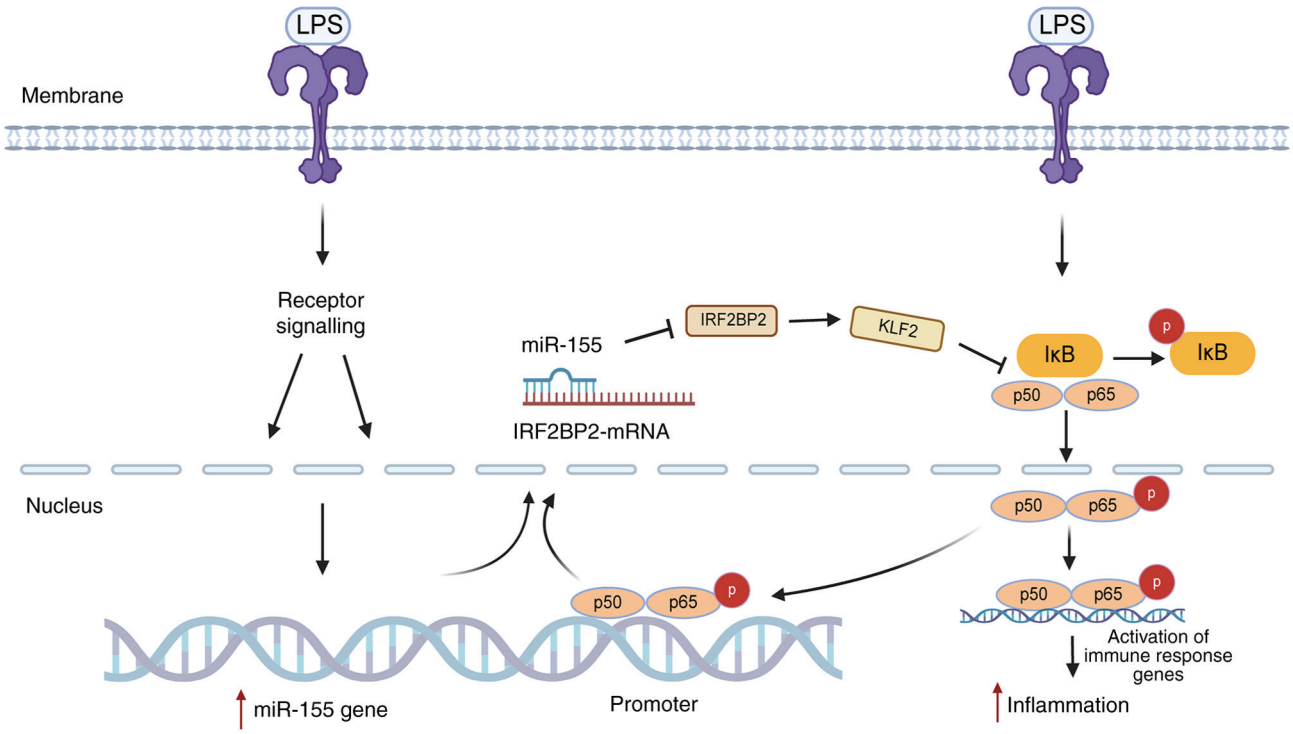

Figure 18. Feedback loop for miR-155. Following LPS stimulation, miR-155 maintains the inflammatory state of psoriasis by targeting the IRF2BP2/KLF2/NF-κB pathway. LPS, lipopolysaccharide; IRF2BP2, IFN regulatory factor 2 binding protein 2; miR, microRNA; KLF2, kruppel-like factor 2; p, phosphorylated.

inflammatory genes and cytokines such as IL-1, IL-8 and TNF-α (42,46,48,49).

According to Masalha *et al* (50), miR-155 exerts a positive feedback function in controlling inflammatory signals. By binding to their receptors, pro-inflammatory cytokines such as IL-1β, IFN-γ, TNF-α and IFN-α trigger inflammatory signals via NF-κB. This increases expression of miR-155 due to NF-κB binding to miR-155 promoter. In addition, miR-155 targets PTEN and suppressor of cytokine signaling 1, two inflammatory signaling inhibitors. The PI3K/AKT pathway, which activates NF-κB, is inhibited by PTEN. Thus, by blocking PTEN via the PI3K/AKT pathway, miR-155 triggers inflammatory and NF-κB signals. Sustained inflammatory signaling results in greater secretion of inflammatory chemokines, increasing the cytokine repertoire at the inflammation site. This increases signaling that activates miR-155 expression, maintaining inflammation in psoriasis (50).

The present study discovered that miR-155 expression was increased in HaCaT cells following LPS stimulation. High miR-155 expression inhibited the target gene, IRF2BP2, leading to decreased expression of KLF2 gene. This weakened the inhibitory effect of the KLF2 anti-inflammatory gene on NF-κB activity. The transcriptional activation domain of p65 was activated, expression of p-p65 protein was enhanced and the activation of NF-κB in the nucleus increased inflammatory factor expression, promoting the inflammatory response of HaCaT cells. Activated NF-κB binds to the miR-155 promoter to increase the expression of miR-155. Thus, a novel positive feedback loop may exist in which miR-155 enhances p-p65 expression via IRF2BP2/KLF2, activates NF-κB, promotes self-expression and maintains the inflammatory state in psoriasis (Fig. 18).

The present study identified miR-155 and IRF2BP2 as potential psoriasis biomarkers. In the LPS-stimulated HaCaT inflammatory cell model, overexpression of miR-155 promoted the inflammatory response, while inhibition of miR-155 attenuated it. Suppression of inflammatory cytokine expression by miR-155-5p inhibitor was reversed by knockdown of IRF2BP2. Mechanistically, miR-155 was shown to regulate inflammation in HaCaT cells via IRF2BP2/KLF2/NF-κB.

In conclusion, based on bioinformatics analysis of clinical samples from patients with psoriasis, the present study confirmed that miRNA-155 decreased IRF2BP2 expression. miRNA-155 also decreased KLF2 expression, which reduced the inhibitory effect of KLF2 on NF-κB transcription activity and increased p-p65 protein expression, thereby increasing expression of inflammatory genes and cytokines. This mechanism results in heightened inflammatory reactions and harm to tissue and keratinocytes and may serve a role in the onset of psoriasis. The results of the present study therefore provide new information on how miR-155 controls development and course of psoriasis.

The present study also had certain limitations. miR-155 inhibitors were not used for dual verification and few psoriasis-associated indicators were detected. Further studies are required to detect psoriasis-associated indicators such as TNF-α, IL-17 and IL-23 and determine whether IRF2BP2 overexpression can reverse the increase of inflammatory cytokines induced by miR-155 mimic.

Acknowledgements

Not applicable.

Funding

The present study was supported by National Natural Science Foundation of China (grant no. 31671092) and The Research Fund of Jianghan University (grant no. 2023KJZX29).

Availability of data and materials

The data generated in the present study may be requested from the corresponding author.

Authors' contributions

WQ and KG conceived and designed the study. LC and XX performed bioinformatics analysis. LC and CL performed the statistical analysis. LC and WQ drafted the manuscript. WQ and KG reviewed and edited the manuscript. LC and WQ confirm the authenticity of all the raw data. All authors have read and approved the final manuscript.

Ethics approval and consent to participate

Not applicable.

Patient consent for publication

Not applicable.

Competing interests

The authors declare that they have no competing interests.

References

1. Boehncke WH and Schön MP: Psoriasis. Lancet 386: 983-994, 2015.
2. Hwang ST, Nijsten T and Elder JT: Recent highlights in psoriasis research. J Invest Dermatol 137: 550-556, 2017.
3. Chiricozzi A, Romanelli P, Volpe E, Borsellino G and Romanelli M: Scanning the immunopathogenesis of psoriasis. Int J Mol Sci 19: 179, 2018.
4. Ciccia F, Triolo G and Rizzo A: Psoriatic arthritis. N Engl J Med 376: 2094-2095, 2017.
5. Griffiths CEM, Armstrong AW, Gudjonsson JE and Barker JNWN: Psoriasis. Lancet 397: 1301-1315, 2021.
6. Dopytalska K, Czaplicka A, Szymańska E and Walecka I: The essential role of microRNAs in inflammatory and autoimmune skin diseases-a review. Int J Mol Sci 24: 9130, 2023.
7. Dopytalska K, Ciechanowicz P, Wiszniewski K, Szymańska E and Walecka I: The role of epigenetic factors in psoriasis. Int J Mol Sci 22: 9294, 2021.
8. Yang SC, Alalaiwe A, Lin ZC, Lin YC, Aljuffali IA and Fang JY: Anti-inflammatory microRNAs for treating inflammatory skin diseases. Biomolecules 12: 1072, 2022.
9. Beer L, Kalinina P, Köcher M, Laggner M, Jeitler M, Abbas Zadeh S, Copic D, Tschachler E and Mildner M: miR-155 contributes to normal keratinocyte differentiation and is upregulated in the epidermis of psoriatic skin lesions. Int J Mol Sci 21: 9288, 2020.
10. García-Rodríguez S, Arias-Santiago S, Blasco-Morente G, Orgaz-Molina J, Rosal-Vela A, Navarro P, Magro-Checa C, Martínez-López A, Ruiz JC, Raya E, *et al*: Increased expression of microRNA-155 in peripheral blood mononuclear cells from psoriasis patients is related to disease activity. J Eur Acad Dermatol Venereol 31: 312-322, 2017.
11. Xu L, Leng H, Shi X, Ji J, Fu J and Leng H: MiR-155 promotes cell proliferation and inhibits apoptosis by PTEN signaling pathway in the psoriasis. Biomed Pharmacother 90: 524-530, 2017.
12. Pastor TP, Peixoto BC and Viola JPB: The transcriptional co-factor IRF2BP2: A new player in tumor development and microenvironment. Front Cell Dev Biol 9: 655307, 2021.
13. Fagerberg L, Hallström BM, Oksvold P, Kampf C, Djureinovic D, Odeberg J, Habuka M, Tahmasebpoor S, Danielsson A, Edlund K, *et al*: Analysis of the human tissue-specific expression by genome-wide integration of transcriptomics and antibody-based proteomics. Mol Cell Proteomics 13: 397-406, 2014.
14. Ma YL, Xia JL and Gao X: Suppressing Irf2bp2 expressions accelerates metabolic syndrome-associated brain injury and hepatic dyslipidemia. Biochem Biophys Res Commun 503: 1651-1658, 2018.
15. Ramalho-Oliveira R, Oliveira-Vieira B and Viola JPB: IRF2BP2: A new player in the regulation of cell homeostasis. J Leukoc Biol 106: 717-723, 2019.
16. Chen HH, Keyhanian K, Zhou X, Vilmundarson RO, Almontashiri NA, Cruz SA, Pandey NR, Lerma Yap N, Ho T, Stewart CA, *et al*: IRF2BP2 reduces macrophage inflammation and susceptibility to atherosclerosis. Circ Res 117: 671-683, 2015.
17. Cruz SA, Hari A, Qin Z, Couture P, Huang H, Lagace DC, Stewart AFR and Chen HH: Loss of IRF2BP2 in microglia increases inflammation and functional deficits after focal ischemic brain injury. Front Cell Neurosci 11: 201, 2017.
18. Feng X, Lu T, Li J, Yang R, Hu L, Ye Y, Mao F, He L, Xu J, Wang Z, *et al*: The tumor suppressor interferon regulatory factor 2 binding protein 2 regulates Hippo pathway in liver cancer by a feedback loop in mice. Hepatology 71: 1988-2004, 2020.
19. Hari A, Cruz SA, Qin Z, Couture P, Vilmundarson RO, Huang H, Stewart AFR and Chen HH: IRF2BP2-deficient microglia block the anxiolytic effect of enhanced postnatal care. Sci Rep 7: 9836, 2017.
20. Li T, Luo Q, He L, Li D, Li Q, Wang C, Xie J and Yi C: Interferon regulatory factor-2 binding protein 2 ameliorates sepsis-induced cardiomyopathy via AMPK-mediated anti-inflammation and anti-apoptosis. Inflammation 43: 1464-1475, 2020.
21. Huang da W, Sherman BT and Lempicki RA: Bioinformatics enrichment tools: Paths toward the comprehensive functional analysis of large gene lists. Nucleic Acids Res 37: 1-13, 2009.
22. Piruzian E, Bruskin S, Ishkin A, Abdeev R, Moshkovskii S, Melnik S, Nikolsky Y and Nikolskaya T: Integrated network analysis of transcriptomic and proteomic data in psoriasis. BMC Syst Biol 4: 41, 2010.
23. Gauthier J, Vincent AT, Charette SJ and Derome N: A brief history of bioinformatics. Brief Bioinform 20: 1981-1996, 2019.
24. Livak KJ and Schmittgen TD: Analysis of relative gene expression data using real-time quantitative PCR and the 2(-Delta Delta C(T)) method. Methods 25: 402-408, 2001.
25. Ni X and Lai Y: Keratinocyte: A trigger or an executor of psoriasis? J Leukoc Biol 108: 485-491, 2020.
26. Xiuli Y and Honglin W: miRNAs flowing up and down: The concerto of psoriasis. Front Med (Lausanne) 8: 646796, 2021.
27. Bartel DP: MicroRNAs: Genomics, biogenesis, mechanism, and function. Cell 116: 281-297, 2004.
28. Guo H, Ingolia NT, Weissman JS and Bartel DP: Mammalian microRNAs predominantly act to decrease target mRNA levels. Nature 466: 835-840, 2010.
29. Jinnin M: Various applications of microRNAs in skin diseases. J Dermatol Sci 74: 3-8, 2014.
30. Wu R, Zeng J, Yuan J, Deng X, Huang Y, Chen L, Zhang P, Feng H, Liu Z, Wang Z, *et al*: MicroRNA-210 overexpression promotes psoriasis-like inflammation by inducing Th1 and Th17 cell differentiation. J Clin Invest 128: 2551-2568, 2018.
31. Raaby L, Langkilde A, Kjellerup RB, Vinter H, Khatib SH, Hjuler KF, Johansen C and Iversen L: Changes in mRNA expression precede changes in microRNA expression in lesional psoriatic skin during treatment with adalimumab. Br J Dermatol 173: 436-447, 2015.
32. Sonkoly E, Wei T, Janson PC, Sääf A, Lundeberg L, Tengvall-Linder M, Norstedt G, Alenius H, Homey B, Scheynius A, *et al*: MicroRNAs: Novel regulators involved in the pathogenesis of psoriasis? PLoS One 2: e610, 2007.
33. Liu Q, Wu DH, Han L, Deng JW, Zhou L, He R, Lu CJ and Mi QS: Roles of microRNAs in psoriasis: Immunological functions and potential biomarkers. Exp Dermatol 26: 359-367, 2017.
34. Luo Q, Zeng J, Li W, Lin L, Zhou X, Tian X, Liu W, Zhang L and Zhang X: Silencing of miR-155 suppresses inflammatory responses in psoriasis through inflammasome NLRP3 regulation. Int J Mol Med 42: 1086-1095, 2018.
35. Liu Y, Zhao X, Li J, Zhou L, Chang W, Li J, Hou R, Li J, Yin G, Li X and Zhang K: MiR-155 inhibits TP53INP1 expression leading to enhanced glycolysis of psoriatic mesenchymal stem cells. J Dermatol Sci 105: 142-151, 2022.

36. Wang H, Zhang Y, Luomei J, Huang P, Zhou R and Peng Y: The miR-155/GATA3/IL37 axis modulates the production of proinflammatory cytokines upon TNF-α stimulation to affect psoriasis development. Exp Dermatol 29: 647-658, 2020.
37. Koeppel M, van Heeringen SJ, Smeenk L, Navis AC, Janssen-Megens EM and Lohrum M: The novel p53 target gene IRF2BP2 participates in cell survival during the p53 stress response. Nucleic Acids Res 37: 322-335, 2009.
38. Liang Y, Zhou Y and Shen P: NF-kappaB and its regulation on the immune system. Cell Mol Immunol 1: 343-350, 2004.
39. Wu J, Ding J, Yang J, Guo X and Zheng Y: MicroRNA roles in the nuclear factor kappa B signaling pathway in cancer. Front Immunol 9: 546, 2018.
40. Alexandrov P, Zhai Y, Li W and Lukiw W: Lipopolysaccharide-stimulated, NF-kB-, miRNA-146a- and miRNA-155-mediated molecular-genetic communication between the human gastrointestinal tract microbiome and the brain. Folia Neuropathol 57: 211-219, 2019.
41. McConnell BB and Yang VW: Mammalian Krüppel-like factors in health and diseases. Physiol Rev 90: 1337-1381, 2010.
42. Jha P and Das H: KLF2 in regulation of NF-κB-mediated immune cell function and inflammation. Int J Mol Sci 18: 2383, 2017.
43. Das M, Lu J, Joseph M, Aggarwal R, Kanji S, McMichael BK, Lee BS, Agarwal S, Ray-Chaudhury A, Iwenofu OH, *et al*: Kruppel-like factor 2 (KLF2) regulates monocyte differentiation and functions in mBSA and IL-1β-induced arthritis. Curr Mol Med 12: 113-125, 2012.
44. Mahabeleshwar GH, Qureshi MA, Takami Y, Sharma N, Lingrel JB and Jain MK: A myeloid hypoxia-inducible factor 1α-Krüppel-like factor 2 pathway regulates gram-positive endotoxin-mediated sepsis. J Biol Chem 287: 1448-1457, 2012.
45. Novodvorsky P and Chico TJA: The role of the transcription factor KLF2 in vascular development and disease. Prog Mol Biol Transl Sci 124: 155-188, 2014.
46. Das H, Kumar A, Lin Z, Patino WD, Hwang PM, Feinberg MW, Majumder PK and Jain MK: Kruppel-like factor 2 (KLF2) regulates proinflammatory activation of monocytes. Proc Natl Acad Sci USA 103: 6653-6658, 2006.
47. Mahabeleshwar GH, Kawanami D, Sharma N, Takami Y, Zhou G, Shi H, Nayak L, Jeyaraj D, Grealy R, White M, *et al*: The myeloid transcription factor KLF2 regulates the host response to polymicrobial infection and endotoxic shock. Immunity 34: 715-728, 2011.
48. Nayak L, Goduni L, Takami Y, Sharma N, Kapil P, Jain MK and Mahabeleshwar GH: Kruppel-like factor 2 is a transcriptional regulator of chronic and acute inflammation. Am J Pathol 182: 1696-1704, 2013.
49. SenBanerjee S, Lin Z, Atkins GB, Greif DM, Rao RM, Kumar A, Feinberg MW, Chen Z, Simon DI, Luscinskas FW, *et al*: KLF2 Is a novel transcriptional regulator of endothelial proinflammatory activation. J Exp Med 199: 1305-1315, 2004.
50. Masalha M, Sidi Y and Avni D: The contribution of feedback loops between miRNAs, cytokines and growth factors to the pathogenesis of psoriasis. Exp Dermatol 27: 603-610, 2018.